UNIVERSITAT DE BARCELONA

Final Degree Project

Biomedical Engineering Degree

Design and Validation of a Mechanical Ventilator for Pandemic Emergencies in Low-Resource Settings Using Commonly Available Components

Barcelona, 11 de Juny de 2025

Author: Joana Ros Alonso

Director and Tutor: Ramon Farré Ventura

Design and Validation of a Mechanical Ventilator for Pandemic Emergencies in Low-Resource Settings Using Commonly Available Components

Abstract

This project introduces the design and validation of a cost-effective mechanical ventilator explicitly developed for emergency use in low-resource settings during pandemics and compassive use. It aims to provide a practical, easy-to-manufacture solution in environments where traditional medical equipment is either unavailable or unaffordable due to logistical, economic, or supply chain barriers. The ventilator is primarily constructed from widely available automotive parts, including windshield wiper motors and bellows.

Two versions of the device were created: one for adults and a smaller, adapted model for neonates. Core ventilation parameters (tidal volume, breathing rate, and airway pressure) can be adjusted using simple mechanical and electrical controls. Performance was evaluated through a series of tests using artificial lung models under various simulated clinical conditions. The results showed consistent delivery of target volumes and pressures, with reliable operation across a range of breathing frequencies.

Although the ventilator is not certified for hospital use, it demonstrates significant potential as an emergency respiratory support tool in humanitarian crises. Its design emphasizes simplicity, affordability, and adaptability, offering a feasible alternative for resource-limited healthcare environments.

Keywords: *mechanical ventilator, low-cost medical device, pandemic response, low-medium income country, emergency ventilation, readily available components, open-source medical design.*

Disseny i Validació d'un Ventilador Mecànic per a Pandèmies en Entorns amb Pocs Recursos Utilitzant Components de Fàcil Accés

Resum

Aquest projecte presenta el disseny i la validació d'un ventilador mecànic de baix cost desenvolupat específicament per a ús d'emergència en entorns amb recursos limitats durant pandèmies i en ús compassiu. L'objectiu és oferir una solució pràctica i fàcil de fabricar en entorns on l'equipament mèdic tradicional no està disponible o resulta inassequible a causa de barreres logístiques, econòmiques o de subministrament. El ventilador està construït principalment amb peces d'automoció àmpliament disponibles, incloent-hi motors de parabrises i manxes.

Es van crear dues versions del dispositiu: una per a adults i una altra, més petita, adaptada per a nounats. Els paràmetres bàsics de ventilació (volum, freqüència respiratòria i pressió) poden ajustar-se mitjançant controls mecànics i elèctrics senzills. El rendiment es va avaluar mitjançant una sèrie de proves amb models de pulmó artificial sota diverses condicions clíniques simulades. Els resultats van mostrar una entrega consistent dels volums i pressions, amb un funcionament fiable en un ampli rang de freqüències respiratòries.

Tot i que el ventilador no està certificat per a ús hospitalari, demostra un gran potencial com a eina de suport respiratori d'emergència en situacions humanitàries. El seu disseny posa èmfasi en la simplicitat, l'accessibilitat econòmica i l'adaptabilitat, oferint una alternativa viable per a entorns sanitaris amb recursos limitats.

Paraules Clau: ventilador mecànic*, dispositiu mèdic de baix cost, resposta a la pandèmia, lpaís de renda baixa o mitjana, ventilació d'emergència, components fàcilment disponibles, disseny mèdic de codi obert.*

Acknowledgments

I would like to express my sincere gratitude to Miguel Ángel Rodríguez for his invaluable support and guidance throughout the practical development of this project. His hands-on assistance in the lab, problem-solving mindset, and constant readiness to tackle challenges made this work possible.

I am also deeply grateful to Professor Ramon Farré for his insightful theoretical contributions, critical feedback, and ongoing support during the review process. His expertise and mentorship have been essential in shaping both the technical and conceptual aspects of this project.

Finally, I extend my appreciation to everyone who contributed directly or indirectly to the completion of this work.

Contents

List of Figures

List of Tables

1 INTRODUCTION

Mechanical ventilators support or substitute the respiratory muscles' function by delivering oxygen (O_2) to the patient during inhalation and removing carbon dioxide (CO_2) during exhalation. While a ventilator does not cure underlying conditions, it stabilizes respiratory function, allowing other treatments to address the primary disease [1].

Globally, respiratory diseases represent a significant public health burden in both high- and low-income countries [2], [3]. Chronic respiratory conditions such as asthma and chronic obstructive pulmonary disease (COPD) are widespread and are further aggravated by air pollution, tobacco use, and biomass fuel burning [4]. These conditions disproportionately affect low- and middle-income countries (LMICs), where healthcare infrastructure and resources are frequently inadequate [5].

The urgency of respiratory support became especially evident during recent global health crises, such as the influenza outbreaks and the COVID-19 pandemic [6]. These emergencies revealed considerable deficiencies in ventilator availability, primarily due to a dependence on complex, specialized medical equipment that is vulnerable to manufacturing disruptions and interruptions in international supply chains [7], [8]. Consequently, many regions, particularly LMICs, experienced critical shortages, emphasizing the urgent need for ventilator designs that prioritize affordability, simplicity, and resilience [9], [10].

Solutions are required to address this pressing challenge. This project aims to design and validate a mechanical ventilator that is explicitly focused on rapid and efficient production and deployment during emergencies, emphasizing its simplicity, cost-effectiveness, and reliance on globally available components.

1.1 Motivation

A small number of manufacturers mainly produce most modern medical systems, relying on specialized components and complex technologies [10].

This supply model is vulnerable to disruption during respiratory disease health crises when the global demand for ventilators can suddenly exceed capacity [11]. In addition, the high cost and technological complexity of conventional ventilators severely limit their accessibility in resource-constrained settings. For many LMICs, these devices remain inaccessible due to financial, logistical, and infrastructural barriers [5], [12].

These limitations motivate the development of an alternative ventilator, one that is reliable, affordable, and easy to operate. The design emphasizes rapid production using widely available components, ensuring suitability for emergency use in low-resource settings.

1.2 Objectives

The primary objective of this project is to design, develop, and validate a positive-pressure mechanical ventilator constructed from commonly sourced, low-cost components, enabling its rapid production during health emergencies in LMICs.

To ensure reliable and effective performance, the ventilator must be capable of delivering adjustable ventilation amplitude and respiratory rates while operating reliably under a range of respiratory conditions with varying airway resistance and lung compliance. During operation, the pressure levels will be continuously monitored to ensure secure ventilation. The design will prioritize the use of basic tools and materials commonly accessible in local contexts, thereby reducing the reliance on complex electronics, sensors or specialized fabrication tools.

1.3 Feasibility

Automotive components are widely distributed worldwide, supported by the industry's extensive supply networks [13]. In many LMICs, the automotive sector represents a significant part of the economy [14], ensuring a stable and accessible inventory of spare parts. However, the project must address key constraints, including limited electrical infrastructure, restricted access to medical-grade oxygen, and deployment in semi-permanent or mobile settings. In such conditions, portable and robust respiratory support devices are essential.

1.4 Scope and Limitations

This project focuses on the design, prototyping, and experimental validation of the mechanical ventilator. The scope encompasses the entire development cycle of the device, from conceptual design and component selection to mechanical assembly, parameter adjustment, and performance testing using artificial lung models under various simulated respiratory conditions.

However, the project does not include clinical testing on human or animal subjects, nor does it pursue formal regulatory certification, as these processes require specialized clinical infrastructure, ethical approvals, and extended timelines that fall outside the project scope.

1.5 Success Criteria

The success of this project is evaluated based on the following functional and practical criteria:

- The ventilator delivers adjustable amplitude and respiratory rates.
- Airway pressure is continuously monitored throughout the operation to ensure patient safety and adequate ventilation.
- The design solely uses widely available, low-cost components to support affordability.
- The prototype can be assembled and maintained using basic tools and skills.

2 BACKGROUND

Mechanical ventilation is crucial in critical care, emergency medicine, and surgery, where it ensures adequate gas exchange and supports recovery from respiratory failure. Understanding the fundamentals of mechanical ventilation, including the physiology of the breathing system and the principles and equations that govern its operation, is essential.

Over time, mechanical ventilation has evolved from early negative-pressure systems to the complex, sensor-driven machines used in modern intensive care units [15].

However, this progress has also highlighted differences in access, particularly in LMICs [16]. In response, there has been growing interest in alternative approaches: open-source hardware, additive manufacturing, and the use of readily available components, which appear as promising strategies for developing functional, low-cost ventilators adapted to resource-limited settings [17], [18].

2.1 History Of Mechanical Ventilation

Early attempts at artificial breathing date back to the 17th century, when Robert Hooke demonstrated how external airflow alone could sustain life by ventilating animal lungs using bellows [19].

However, the first practical mechanical ventilators did not appear until the 19th century [20].

These early devices operated on negative pressure, enclosing the entire body in airtight boxes where pressure was manually cycled to facilitate breathing.
Figure 1 illustrates the original iron lung design and its operation during the poliomyelitis epidemics from 1930 to 1950. The iron lung worked by lowering the pressure around the patient's body, expanding the chest and thus triggering inhalation, followed by a return to atmospheric pressure for exhalation [20].

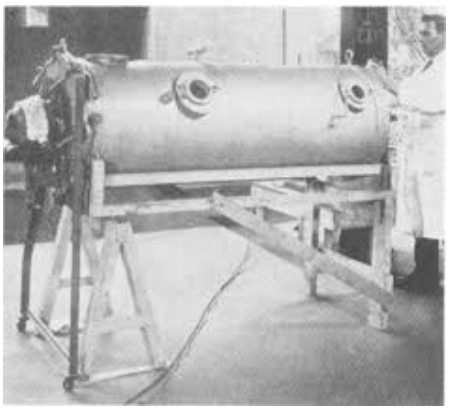

Figure 1. *The "iron lung" negative-pressure ventilator was developed in 1929 by Drinker and Shaw. It enclosed the patient's body in a sealed chamber to simulate natural breathing by cyclically varying the surrounding pressure [21].*

While they were life-saving, this approach caused discomfort and complications, such as reduced cardiac output due to venous pooling in the lower torso.

By the mid-20th century, positive-pressure ventilation emerged as a superior method. Developed during and after World War II, based on principles used in military aviation, such as pressurized oxygen systems for fighter pilots, the introduction of safe endotracheal tubes allowed pressure to be applied directly to the lungs, delivering air volume efficiently [20].

Its adoption began during the polio epidemics of the early 1950s, in the Copenhagen polio outbreak, where clinicians used tracheostomies and hand-operated bag-valve devices to deliver positive-pressure ventilation. This dramatically improved survival rates and marked a turning point in respiratory care by substituting negative-pressure devices [22], [23].

Over the subsequent decades, mechanical ventilators became a core component of critical care [24].

Early positive-pressure ventilators were pneumatically driven or basic electronically controlled pumps. Modern developments have made ventilators more compact, sophisticated, and responsive [20].

The implementation of microprocessor-controlled systems has allowed the precise delivery of breathing cycles in various modes, with real-time monitoring and feedback control of pressure, volume, and airflow. Moreover, these systems have been equipped with numerous sensors and electronics to adapt ventilation to patient needs and to enhance safety [20]. To design effective ventilators, it is critical to understand the underlying physiology of the respiratory system.

2.2 Fundamentals of Breathing Physiology

Mechanical ventilation supports or replaces the body's natural breathing process when spontaneous respiration is impaired. Effective breathing is essential to fill alveoli with new air, allowing oxygen to diffuse into the blood and removing carbon dioxide [25].

Under physiological conditions, spontaneous breathing occurs through the generation of cyclical negative pressure inside the thorax, followed by passive elastic recoil (Figure 2) [25].

Inhalation is initiated by the contraction of the diaphragm and the external intercostal muscles, which expands the thoracic capacity and increases the intrathoracic volume. This expansion lowers the intrapulmonary pressure below the atmospheric pressure, allowing air to flow into the lungs until equilibrium is reached [26], [27].

During exhalation, the reverse process occurs. The respiratory muscles relax, and the lungs and chest wall return to their resting state through elastic recoil. The decrease in thoracic volume elevates intrapulmonary pressure above atmospheric levels, driving air out of the lungs until alveolar and atmospheric pressures are equalized again [27].

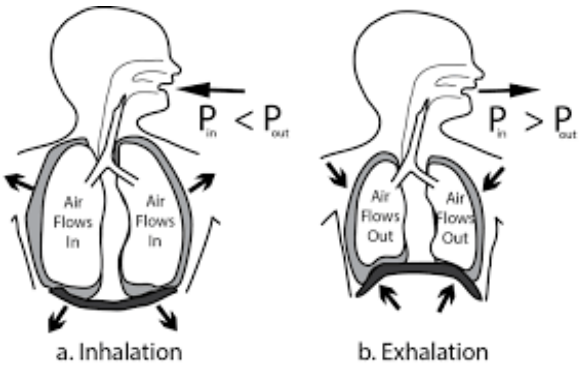

Figure 2. *Mechanics of spontaneous breathing. During inhalation (a), contraction of the diaphragm and expansion of the thoracic cavity lowers intrathoracic pressure, drawing air into the lungs. During exhalation (b), muscle relaxation and elastic recoil raise intrathoracic pressure, pushing air out [28].*

2.2.1 Resistance and Compliance

The effectiveness of this process is mainly affected by two mechanical properties: lung compliance and airway resistance.

Compliance is the distensibility of the lungs and thoracic cage. It describes the volume change that occurs for a given pressure change. It is defined as the change in volume per unit change in pressure. A highly compliant lung requires only a slight pressure drop to inhale a large volume, whereas a low-compliance lung is stiffer and requires larger pressure changes [29], [30]. In healthy adults, the lungs and chest wall have substantial compliance, enabling effortless breathing; diseases like pulmonary fibrosis reduce compliance (stiffening the lungs), making inhalation more difficult.

Airway resistance, mainly caused by air viscosity, refers to the opposition to airflow within the respiratory tract. It is quantified as the pressure difference needed to achieve a specific flow rate (pressure per unit flow) [27], [31]. Higher resistance (for example, due to bronchoconstriction or mucus plugging in the airways) requires more pressure to be generated to deliver the same airflow, thereby increasing the work of breathing [27].

2.2.2 The model of breathing

The mechanical behavior of the respiratory system can be described using the equation of motion for the lung, which models the balance of forces involved in ventilation [32]:

$$P_{mus} + P_{vent} = P_{el} + P_{res} \quad (1)$$

where:

- P_{mus}: Muscular pressure generated by the patient's respiratory muscles. (cmH_2O)
- P_{vent}: Ventilator pressure applied by the MV to assist or control breathing. (cmH_2O)
- P_{el}: Elastic recoil pressure of the lung and chest wall, due to their compliance. (cmH_2O)
- P_{res}: Resistive pressure required to overcome airway resistance to gas flow. (cmH_2O)

or, using measurable variables:

$$P(t) = R \cdot V'(t) + \frac{V(t)}{C} \quad (2)$$

where:

- *P(t)*: Total pressure applied to the respiratory system. (cmH_2O)
- *R*: Airway resistance. ($cmH_2O \cdot s/L$)
- *V'(t)*: Flow rate. (L/s)
- *V(t)*: Volume delivered to the lungs. (L)
- *C*: Lung compliance. (L/cmH_2O)

$R \cdot V'(t)$ represents the resistive pressure proportional to airflow and airway resistance. In contrast, $V(t)/C$ is the elastic recoil pressure, which increases with lung volume and inversely with compliance.

Equation 2 illustrates how mechanical ventilators must be tuned to accommodate each patient's respiratory mechanics. In patients with stiff lungs (low compliance), higher pressure must be delivered for the same volume. Similarly, for increased airway resistance from obstructive lung diseases, more pressure is required to maintain airflow.

Ventilators must generate enough positive pressure to overcome both types of opposition and support or replace the patient's respiratory effort [33].

2.2.3 Parameters Control

To safely and effectively ventilate a patient, key parameters must be controlled and monitored. The core settings include tidal volume, airway pressure, and respiratory rate, each of which has a specific role in ensuring adequate gas exchange and preventing lung injury. These variables are closely interrelated and are typically adjusted based on the patient's clinical condition and lung mechanics.

2.2.3.1 Minute Ventilation

Minute ventilation refers to the total volume of air exchanged per minute, which influences CO_2 removal and O_2 renewal. It is calculated as the product of tidal volume by respiratory rate.

Higher minute ventilation increases total ventilation and promotes CO_2 clearance. In contrast, a lower one permits more time for each breath and can aid oxygenation by prolonging the inspiratory and expiratory phases if needed.

2.2.3.1.1 Tidal Volume

The tidal volume (VT) is the air delivered to the patient's lungs with each breath. An appropriate tidal volume must be set to ensure sufficient alveolar ventilation without over-distending the lungs. Low VT can lead to hypoventilation and CO_2 retention (hypercapnia), while excessive volumes can cause lung injury from overexpansion (volutrauma) [34]. In adult patients, a typical setting is around 6–8 mL of air per kilogram of ideal body weight [34]; in patients with acute respiratory distress syndrome (ARDS), even lower tidal volumes (4–6 mL/kg) are recommended to minimize barotrauma [35]. Pediatric patients or neonates require appropriately smaller absolute volumes. The tidal volume setting is always balanced against the respiratory rate to maintain adequate minute ventilation.

2.2.3.1.2 Respiratory Rate

The respiratory rate (frequency) is the number of breaths delivered per minute by the ventilator. In normal resting adults, the physiological breathing rate is about 12–20 breaths per minute. On ventilators, the set rate may range from as low as 10–12 breaths per minute in an adult to 24 breaths per minute or higher frequencies for pediatric cases, reaching 45 breaths per minute [34].

This rate is adjusted based on metabolic demand and blood gas results. Increases may be used to correct respiratory acidosis, but excessively high rates risk incomplete exhalation and air trapping, particularly in patients with obstructive lung conditions. Therefore, carefully balancing rate, volume, and inspiratory/expiratory timing is essential [29].

2.2.3.2 Airway Pressure

This refers to the pressure within the central airways during ventilation, resulting from gas flow and lung/chest wall recoil. In mechanical ventilation, airway pressure has to be controlled and monitored. Key pressure parameters include the peak inspiratory pressure (highest pressure during breath delivery) and the plateau pressure (the pressure in the lungs during an end-inspiratory pause, reflecting alveolar pressure) [36]. Additionally, a baseline positive end-expiratory pressure (PEEP) is often applied to prevent alveoli from collapsing at end-expiration, thereby improving oxygenation [37]. Maintaining appropriate airway pressures is essential for avoiding injury; excessive pressures can lead to barotrauma.

2.3 Enabling Technologies

High cost, proprietary design, and a complex regulatory landscape characterize the conventional medical device industry. While these measures ensure safety and quality, they also create significant barriers to access, particularly in LMICs or during global crises. In response, open-source hardware and repurposed components have emerged as enabling tools for developing functional, low-cost medical solutions [38], [39]. These approaches form the foundation of the ventilator proposed in this project, which aims to provide a practical, accessible solution for emergency use in resource-limited settings.

2.3.1 Open-Source Hardware (OSH)

Open-source hardware provides publicly accessible design files under licenses that allow anyone to study, modify, and reproduce the device. This collaborative model encourages rapid innovation, continuous improvement, and local adaptation [40]. Several ventilator development efforts in recent years have embraced OSH principles, aiming for transparency, affordability, and adaptability [38]. By removing the constraints of proprietary design, open-source ventilators can be tailored to local needs, manufactured with accessible tools, and improved by a global community of contributors.

2.3.2 Readily Available Components

Another key strategy involves using off-the-shelf industrial components, which are often more affordable and easier to source than certified medical-grade parts. This is especially important in LMICs, where global supply chains may be disrupted or prohibitively expensive.

As shown in this project, components such as windshield wiper motors, air suspension bellows, or standard relays can be repurposed to create ventilators that are not only low-cost but also easier to assemble, maintain, and repair. This approach supports resilience, decentralized production, and long-term sustainability in resource-constrained environments.

2.4 Literature Review

The COVID-19 pandemic temporarily increased the global demand for intensive care mechanical ventilation capacity. While ICUs were under immense pressure globally, several high-income countries (HICs) did not ultimately require novel prototype ventilators, as standard ventilator supplies were sufficient to meet demand [41]. In contrast, mechanical ventilation capacity was, and largely remains, insufficient in the vast majority of LMICs, limiting access to critical care and surgery.

In response to the COVID-19 pandemic, some non-governmental organizations began work on designing ventilators for LMICs. Several open-source ventilators were developed. Some projects have been selected to illustrate the different design strategies and component choices [38], [39].

2.4.1 AmboVent

The AmboVent ventilator [42] is an open-source emergency device engineered for low-cost mass production using off-the-shelf components. It relies on a manual resuscitator bag (Ambu bag) as the core element for delivering breaths. An Arduino Nano microcontroller governs a motor-driven linkage that rhythmically compresses the Ambu bag. At the same time, dial potentiometers allow the operator to set parameters such as tidal volume (by adjusting the compression depth), respiratory rate, and maximum inspiratory pressure.

2.4.2 ApolloBVM

The ApolloBVM [43] is another low-cost automated ventilator based on an Ambu bag. As shown in Figure 3, the ApolloBVM uses a dual rack-and-pinion mechanism driven by an electric motor to compress a standard BVM from both sides simultaneously. The device's control system is built around two Arduino Uno microcontrollers directing the motors and sensors.

The frame and mechanical parts of ApolloBVM were designed for rapid fabrication; the prototype was primarily built from laser-cut plywood and 3D-printed components, enabling quick scaling and assembly.

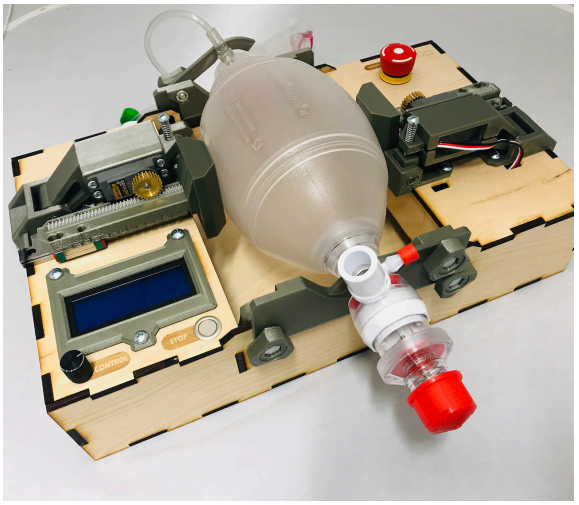

Figure 3. *ApolloBVM: low-cost, open-source ventilator using a dual rack-and-pinion mechanism. Built primarily from laser-cut plywood and 3D-printed components [44].*

2.4.3 MIT E-Vent

The MIT E-Vent project was launched in early 2020. Like the above designs, it uses a BVM (Ambu bag) as the breathing unit, which is compressed by a mechanical actuator (in MIT's design, a pair of motor-driven paddles) to simulate the action of hand ventilation. The system provides basic controlled ventilation modes; specifically, it can operate in a volume-controlled ventilation mode where the user sets the tidal volume, inspiratory/expiratory ratio, and breaths per minute. The MIT E-Vent incorporates essential safeguards, including an adjustable pressure-relief valve and a Positive End-Expiratory Pressure (PEEP) valve on the breathing circuit.

2.4.4 Mechanical Ventilator Milano (MVM)

In contrast to the Ambu bag compressors described above, the MVM [45] is a pneumatic ventilator (Figure 4). Instead of squeezing a bag, it uses solenoid valves to control the gas flow from a pressurized source to the patient. Using industrial solenoid valves, pressure transducers, and microcontroller-based control electronics, the ventilator was designed in a modular format to permit individual component substitution. This allowed for two distinct ventilation modes: a full mandatory ventilation mode and a gentler assisted breathing mode.

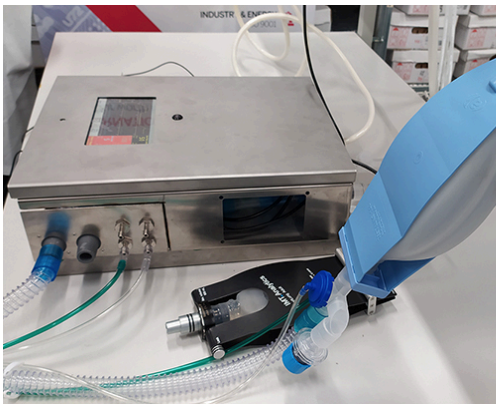

Figure 4. *MVM: pneumatic open-source ventilator using industrial solenoid valves to regulate gas flow. Designed with modular, swappable parts [46].*

2.4.5 Supply Chain Considerations

While these open-source ventilator projects show low-cost, modular designs that can be rapidly produced, they also share a critical dependency on modern supply chains. Each device requires key electronic and mechanical components (such as microcontroller boards, motor drivers, stepper motors, sensors, and valves) or non-electronic components, like the Ambu Bag, which may become scarce during a global crisis. A pandemic not only increases demand for such parts but can also disrupt manufacturing and exports. Even widely used items like Arduinos or pressure sensors can be challenging to procure when factories are shut down, or stock is diverted to high-income markets. Moreover, ventilator designs that are not flexible about part substitutions can stall if any one item on the bill of materials is unavailable. Thus, the general availability of these open-source ventilators in a global emergency context is limited by the weakest link in their component supply.

3 MARKET ANALYSIS

The ventilator market is mature and competitive, yet low-cost options are underrepresented. The COVID-19 pandemic highlighted and exacerbated this gap, underscoring the pressing need for cost-effective ventilators in global healthcare systems [47].

3.1 Market Overview

The global mechanical ventilator market is experiencing significant growth. Aging populations, the increasing prevalence of respiratory diseases, and the impact of the COVID-19 pandemic are contributing factors [48].

3.1.1 Global Demand and Supply

The mechanical ventilators market is expected to register a CAGR of 7.5% during the forecast period (2022 - 2027) [49]. Before the COVID-19 pandemic, market growth was driven by an aging population and an increase in respiratory diseases. However, the pandemic caused an unprecedented surge in demand, with manufacturers struggling to meet global needs [48]. As shown in Figure 5, the ventilator market experienced a significant spike during the COVID-19 pandemic, with projections indicating steady growth through 2030.

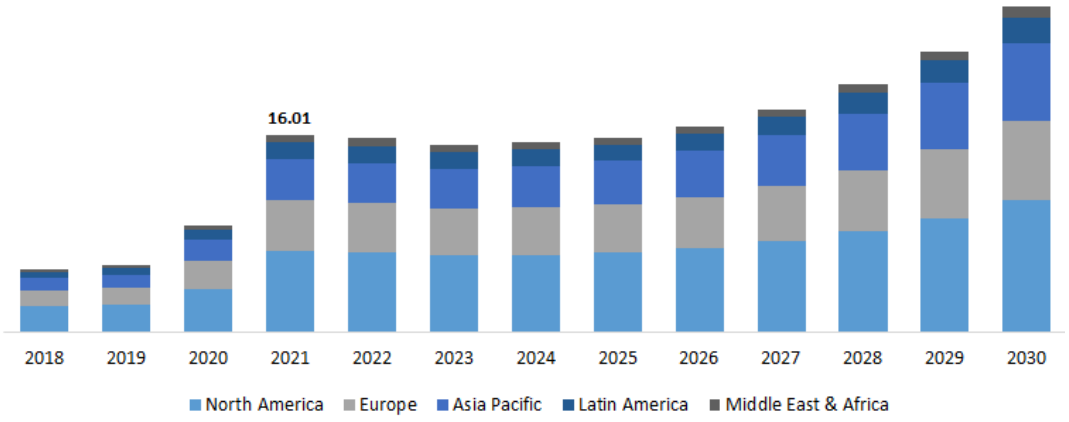

Figure 5. *Global ventilator market size by region, 2018–2030 (USD billion). The chart shows a sharp increase in 2020–2021 due to the COVID-19 pandemic, followed by continued growth across all major regions, particularly North America and Asia Pacific. [50]*

3.1.2 Impact of COVID-19

The COVID-19 outbreak positively impacted the mechanical ventilators market due to their increased use in managing the disease [48]. The pandemic exposed critical gaps in ventilator availability, especially in LMICs. Countries worldwide experienced shortages of ventilators,

prompting government interventions, increased production, and innovation. The market has stabilized post-pandemic but remains shaped by the effects [48].

This surge in demand is expected to persist in the coming years, driven by the projected increase in chronic diseases. Moreover, the pandemic accelerated the development of alternative ventilator designs, including emergency-use devices, open-source projects, and repurposed equipment. Governments and healthcare providers were forced to rethink procurement strategies and prioritize adaptability and scalability.

3.2 Market Drivers and Restraints

Several critical drivers and challenges influence market dynamics, shaping the demand for mechanical ventilators. These factors collectively contribute to the growing need for innovative, accessible ventilator solutions.

3.2.1 Key Market Drivers

- **Aging population:** The global increase in the elderly population significantly drives demand for ventilators. In developed countries, life expectancy has doubled over the past two centuries, with those over 65 projected to comprise about 20% of the population by 2050 [51]. As people age, their respiratory systems undergo changes that reduce lung elasticity and weaken respiratory muscle function, leading to a higher incidence of respiratory illnesses that require ventilatory support [52].
- **Prevalence of chronic respiratory diseases:** The rising incidence of chronic respiratory diseases, including chronic obstructive pulmonary disease (COPD), asthma, and acute respiratory distress syndrome (ARDS), drives ventilator demand globally. Air pollution, smoking, and industrialization have led to an increase in cases of these conditions, often requiring prolonged ventilatory support, particularly in severe stages [53].
- **Impact of environmental factors on respiratory health:** Industrial emissions, vehicle exhaust, and indoor pollutants contribute to the development and worsening of respiratory illnesses. Populations in high-pollution areas experience a higher prevalence of respiratory conditions that may necessitate ventilator support, especially during acute exacerbations [54].
- **Technological advancements in ventilator design:** Recent advancements in ventilator technology, including portable and home-use ventilators, are expanding market reach and accessibility. Innovations in ventilator design, such as non-invasive ventilators and user-friendly interfaces, have broadened the scope of ventilator applications beyond traditional hospital settings, making respiratory care more accessible [39], [55].
- **Climate change and air quality:** Climate change is increasingly recognized as a significant contributor to respiratory illnesses worldwide. Rising temperatures and altered weather patterns increase ground-level ozone, prolong pollen seasons, and contribute to more frequent and intense wildfires. These changes degrade air quality and lead to

higher incidence and severity of respiratory diseases, increasing the demand for ventilatory support [56], [57].

At the same time, there are notable barriers that limit the widespread adoption and effective deployment of ventilators, particularly in low-resource settings.

3.2.2 Challenges and Restraints

- **High production and maintenance costs:** Mechanical ventilators are expensive due to the use of specialized materials and intricate assembly processes. These high cost significantly limits, particularly in LMICs. Moreover, maintenance expenses add to the financial burden on healthcare facilities [58].
- I**nfrastructure limitations in LMICs:** The lack of necessary infrastructure to support advanced ventilators, including reliable electricity, stable oxygen supplies, and sufficient space for equipment, is a constraint in LMICs. These limitations often make even donated ventilators challenging to operate and maintain, reducing their overall utility in such settings [59].
- **Shortage of skilled operators and maintenance technicians:** Operating mechanical ventilators requires trained healthcare staff skilled in handling and troubleshooting the device. A shortage of such personnel leads to under-utilization or misuse of ventilators. The lack of qualified technicians also increases device downtime and faster degradation, as minor issues may go unaddressed until they become significant problems [58].
- **Supply chain vulnerabilities and component shortages:** The COVID-19 pandemic exposed significant vulnerabilities in the ventilator supply chain, resulting in critical component shortages that caused delays and impacted production capacity. Global supply chain disruptions have made it difficult for manufacturers to meet surging demands, and these challenges persist in times of increased demand, highlighting an ongoing risk to ventilator availability [59].

3.3 Competitive Landscape

A mix of long-established medical technology firms and specialized respiratory care companies dominates the global ventilator market. These players compete on the basis of technological innovation, production capacity, and geographic reach.

3.3.1 Key Market Players

The ventilator market is highly competitive. Some of the prominent players profiled include Getinge AB, Medtronic, Vyaire Medical Inc., Drägerwerk AG & Co. KGaA, Koninklijke Philips N.V., Hamilton Medica*l, GE Healthcare, ICU Medical, Inc., ZOLL Medical Corporation, and Mindray.* [60], [61].

3.3.2 COVID-19 Responses by Major Companies

During the peak of the COVID-19 pandemic, several manufacturers ramped up production to meet the increased demand for ventilators. This disrupted worldwide supply chains, causing shortages of critical medical equipment, electronics, and raw materials.

For instance, in March 2020, Zoll Medical Corporation implemented a plan to increase manufacturing capacity to 10,000 ventilators per month in response to the COVID-19 pandemic, representing almost a 25-fold expansion from recent production volumes. In March 2020, Philips expanded ventilator production at a U.S. facility, scaling output to approximately 4,000 units per week by the third quarter of 2020. It also launched the emergency-use Respironics E30, producing up to 15,000 units weekly to meet urgent global demand [62].

In January 2021, Inovytec entered a deal to supply 1,500 progressive portable ventilators to Italy, Brazil, and Israel. It agreed with a California-based distributor to provide the ventilators, which may assist patients with respiratory illnesses during the COVID-19 pandemic and beyond [63].

3.4 Opportunities for Innovation

The availability and accessibility of mechanical ventilators remain critical public health concerns globally, particularly in LMICs. Standard ventilators typically cost around $ 20,000, making them prohibitively expensive, even for many developed countries, and severely limiting access in resource-constrained regions [64], [65]. This significant market gap highlights an urgent need for affordable, robust, and easily maintainable ventilator solutions that leverage locally available components and simplified manufacturing processes. Such conditions present substantial opportunities for innovation, especially for new market entrants capable of developing context-appropriate technologies tailored to the specific infrastructure limitations and economic realities of LMICs.

In response to this opportunity, the present project proposes developing a mechanical ventilator utilizing readily available automotive components. The resulting ventilator aims to provide a cost-effective, sustainable, and easily maintainable solution, ideally suited for rapid deployment and prolonged use in resource-limited settings by harnessing the extensive and globally distributed automotive supply chains.

4 CONCEPTUAL ENGINEERING

To achieve the desired objective, a comprehensive study was conducted to evaluate viable design solutions for the mechanical ventilator. All selected components were chosen based on their functional adequacy, cost-effectiveness, and, most critically, global availability.

In some instances, optimal performance was intentionally traded off in favor of affordability and practical sourcing, particularly by emphasizing parts from the automotive industry, where standardization and widespread distribution offer key advantages.

4.1 Functional Requirements

The primary clinical requirement for this ventilator is to provide respiratory support. Technically, it must rely on readily available, low-cost automotive components to ensure accessibility, particularly in low-resource and emergency settings. Additional constraints include easy assembly, intuitive operation, and minimal dependence on specialized infrastructure or maintenance.

Two distinct ventilator designs were developed: one for adults and one for neonates.

The adult ventilator was designed to deliver higher tidal volumes at lower frequencies, while the neonatal version prioritized compactness and higher-frequency operation with smaller volumes.

Both systems are required to generate sufficient airway pressure to overcome the elevated resistance and reduced lung compliance commonly seen in adult patients with obstructive or restrictive conditions, as well as in neonates with naturally low lung compliance.

4.2 Analysis Selection of Critical Components

The key mechanical and pneumatic elements of the ventilator are evaluated against the established functional requirements, focusing on the selection of an appropriate actuator (motor) and then on the design of the air chamber.

Each component is compared in terms of availability, performance, and ease of local sourcing. The goal is to ensure that the final design can reliably meet both adult and neonatal ventilation needs while remaining low-cost and easily serviceable.

4.2.1 Motor

The windshield wiper motor was the only actuator considered for the ventilator design, as it met all the required performance characteristics and was easily accessible.

Since its mechanism is standardized across all automobiles, the design does not depend on a specific brand or model, allowing for adaptability using locally sourced components.

- **Front windshield wiper motor** (selected for adult ventilator): This motor provides moderate rotational speed and higher torque (power), which is suitable for the required adult ventilatory frequencies and larger tidal volumes. Its robust structure ensures stable and consistent operation under higher loads.
- **Rear windshield wiper motor** (selected for neonatal ventilator): This motor offers higher rotational speed but lower torque, with a compact and lightweight design, making it appropriate for the lower volumes and higher frequencies necessary in neonatal ventilation.

4.2.2 Air Chamber

Several automotive bellows were assessed based on elasticity, durability, and internal volume; for the presented prototypes, the ones selected were:

- **CV joint bellows** (selected for adult ventilator): Selected because of its elasticity, durability, and ease of compression, with an internal volume of approximately 600 cm^3 per unit. Two bellows were configured in parallel to meet adult ventilatory requirements (approximately 800 cm^3 tidal volume), achieving scalable modularity and adequate capacity.
- **Inner tie rod boot** (selected for neonatal ventilator): This boot is characterized by high elasticity, compact size, and a lower internal volume (approximately 350 cm^3), making it suitable for neonatal ventilation where lower tidal volumes are required.

4.3 Analysis of Alternative Solutions

Table 1 summarizes the considered options for both the motor and bellows.

Component	Alternative	Pros	Cons	Selection
Motor	Front wiper motor	Adequate torque for adults, wide availability	Larger size	Yes. For adult's version
	Rear wiper motor	Compactness and availability	Lower subjection and robustness. Overheating	Yes. For neonatal version
Air Chamber	Air suspension bellows	Structural robustness, adequate volume, and pre-made holes	Excessive stiffness	No
	CV Joint bellows	Soft, durable, easy deformation	Slightly low volume and prone to lateral deformation	Yes. For adult's version
	Drawbar gaiter	Durable and good axial deformation		No. Option for further versions
	Inner tie rod boot	Compact size	Smaller volume	Yes. For neonatal version
	Dual-stage bellows	Good articulation	Unpredictable deformation	No

Table 1. *Comparison of motor and bellows alternatives evaluated during the conceptual design phase.*

5 DETAILED ENGINEERING

The working mechanism of the compression system and pressure monitor are described in detail in this section. Once assembled, all the functionalities were systematically tested, and the results are presented, showing the variable volume with its maximums and minimums for both the adult and newborn MV versions.

5.1 Motor and Actuation System

The actuation system begins with a standard automotive windshield wiper motor chosen for its wide availability, mechanical robustness, and built-in gear reduction. This motor, along with its original linkage mechanism, was mounted onto a wooden support base, with the linkage secured using screws. The original rubber bushings in the linkage were deliberately preserved, serving to absorb mechanical shocks and minimize vibration transfer to the structure

Internally, the wiper motor contains a high-speed DC motor that spins at approximately 2500–3000 revolutions per minute (rpm) under no-load conditions [66]. However, due to its integrated gear reduction system, the output is dramatically slowed down to produce an oscillatory motion at approximately 40–60 cycles per minute [67], which aligns well with the typical frequency range required for mechanical ventilation. As illustrated in Figure 6, the rotating drive axle moves a set of link rods, converting the motor's rotary motion into a reciprocating linear motion. This mimics the sweeping motion used in windshield wiper systems but is repurposed here to compress the ventilator's air chamber.

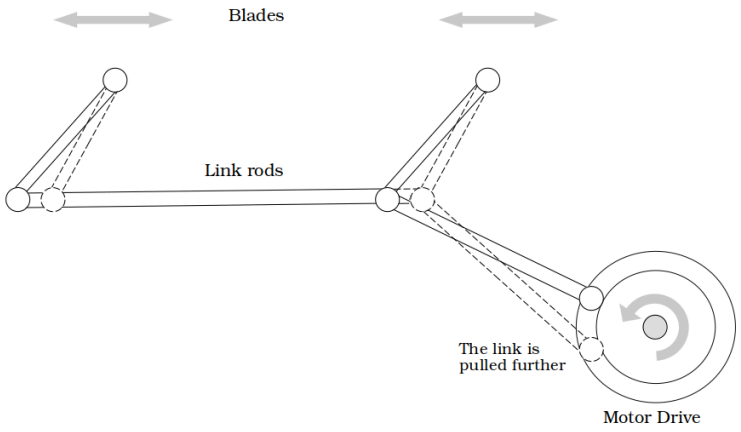

Figure 6. *Internal linkage mechanism converting rotary motion into the movement of the blades.*

The wiper motor is designed to operate at a nominal voltage of 12 V. Its speed is regulated via Pulse Width Modulation (PWM), which adjusts the duty cycle of a high-frequency signal to control

the adequate power delivered to the motor [68]. This allows the blades to move at different speeds: slow for light rain and fast for heavy downpours, without changing the supply voltage.

However, the DC motor speed responds proportionally to changes in voltage. This allows for smooth and continuous adjustment of the actuation frequency to suit different ventilation requirements. In this prototype, the motor speed has been effectively modulated by adjusting the input voltage.

5.2 System Assembly and Integration

The air compression system is built around the bellows, which are responsible for generating airflow into the patient circuit. They are made of flexible, pneumatic-grade rubber and are designed to withstand continuous mechanical deformation. Its accordion-style geometry enables smooth expansion and contraction, returning to its original shape after each cycle without permanent deformation. To achieve the required tidal volume for adult ventilation, two CV (Constant Velocity) joint bellows were mounted in parallel and actuated simultaneously using a shared mechanical linkage. Early tests with a single bellows confirmed basic functionality, but the final configuration doubled the capacity while maintaining structural simplicity.

A rigid connector links both bellows to the actuation mechanism, ensuring balanced force distribution during compression and simultaneous movement. The bellows are sealed at both ends with caps. One end features a cylindrical plug to secure the linearization rod, while the other includes a hollow outlet to connect with the airflow tubing. To reduce leakage, joints are reinforced with steel ear clamps and sealed with silicone. The bellows are aligned horizontally with the motor to ensure correct actuation geometry.
To secure the bellows during compression, a T-shaped support structure was used. It holds the bellows in place and provides a physical stop to limit their maximum deformation.

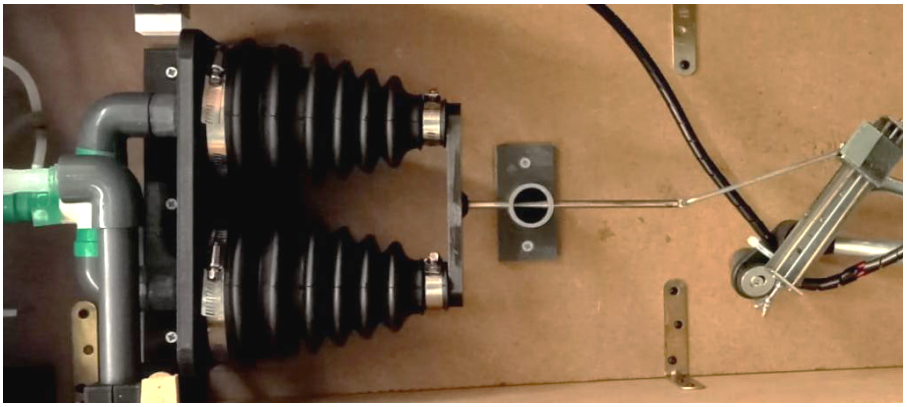

Figure 7. *View of the two CV bellows mounted in parallel. They are fixed to a 3D-printed support structure and connected to the airflow tubing system. On the left, the central linearization rod evenly distributes the compressive force to both bellows, enabling synchronized actuation and increased tidal volume.*

5.3 Linearization Mechanism

The rotational movement of the motor drive needs to be linearized. A custom linearization mechanism was developed to achieve it. While such mechanisms are common in industrial settings, they are not typically found in automotive or household devices, so a simplified, low-cost solution was developed using basic materials.

A two-link articulated system was assembled and implemented to linearly compress and expand the bellows. The mechanism, as illustrated in Figure 8, consists of two rigid steel rods: one bent into a U-shape with 90-degree corners and the other a straight linkage that transmits the force to the actuation point.

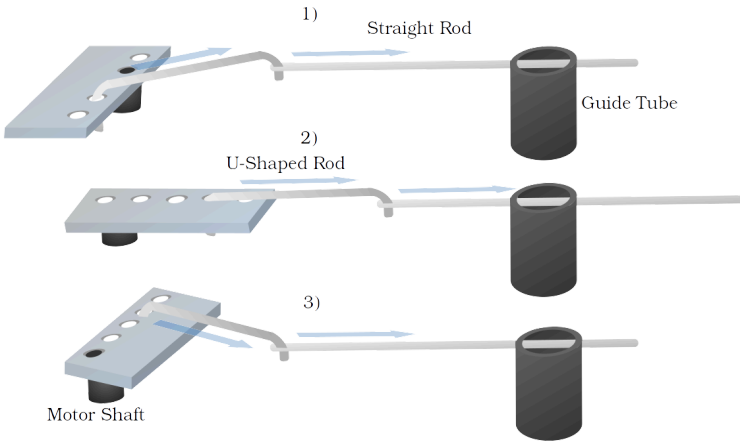

Figure 8. *The linearization mechanism's motion sequence shows three key articulated linkage positions. (2) Maximum compression, zero angle between the rods, (1) and (3) Bellows extension. The U-shaped rod connects the motor-mounted crank plate to the straight rod, which transmits motion through a PVC guide to the bellows. The Stroke amplitude depends on the radial hole selected on the crank plate, affecting the air volume displaced.*

As shown in Figure 8, the U-shaped rod is anchored at one end to a perforated stainless-steel plate mounted on the motor shaft. The plate includes a series of equally spaced holes (1 cm apart), allowing the axis distance to be manually adjusted between 2 cm and 9 cm by inserting and pulling the bent rod from one hole to another. The selected attachment point defines the stroke amplitude and the volume of air displaced in each actuation cycle.

The opposite end of the U-rod and the straight rod are connected via a pivot joint that allows rotational freedom while maintaining structural stability. The straight rod spans the distance to the actuation point between the two CV joint bellows, compressing them symmetrically. The rod passes through two holes drilled into a PVC guide tube to constrain lateral motion. While lower-friction materials, such as nylon, could improve performance, PVC was selected due to its

availability and satisfactory mechanical properties. A grease was applied to reduce friction and ensure smooth motion. A simple animation was created to illustrate the linearization mechanism.

Although the linear motion is well-defined, CV joint bellows do not behave like ideal pistons. They expand and contract through accordion-like folds, introducing non-linearities in the relationship between stroke and expelled air volume. While the motion of the centerline can be approximated as linear, the actual volume change may be slightly nonlinear due to wall elasticity and variable cross-section. Nevertheless, within the tested displacement range, a consistent correlation between stroke amplitude and volume expelled was observed, validating the use of the position as a control parameter.

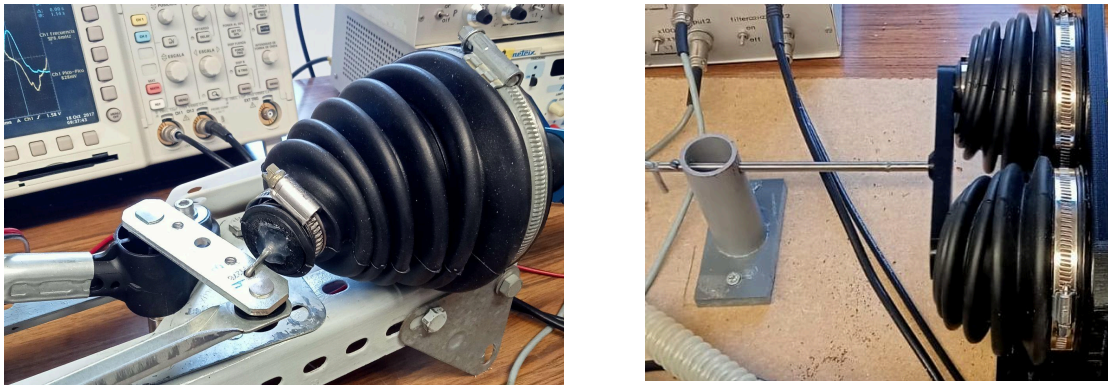

A *B*

Figure 9. *(A) Ventilator setup without a linearization mechanism, showing a single bellow directly actuated by the motor, with some lateral deformation at low compression, which increases during higher tidal volume deliveries. (B) The ventilator is equipped with a linearization mechanism, and two bellows are connected in parallel, allowing for synchronized actuation and enhanced volume delivery.*

5.4 Valves

Two valves, one for inspiration and one for expiration, were integrated into the ventilation system to ensure proper airflow and continuous air renewal. These valves control the direction of air through the circuit, preventing undesired backflow and enabling reliable respiratory cycling.

The inspiratory valve, positioned at the inlet, is a commercial Hans Rudolph bidirectional valve typically used in hospital respiratory circuits. It ensures fresh ambient air is drawn into the bellows during the inspiration phase when negative pressure is generated. In contrast, the expiratory valve, located downstream, is a custom-fabricated component made using a thin latex membrane cut from standard gloves. This handmade valve is a flexible flap: the latex is fixed around its edges, leaving the center free to act as a pressure-sensitive membrane. When positive pressure builds during the expiration phase (as the bellows compress), the membrane deforms and opens to allow air release. The membrane reseals once the pressure equalizes or reverses, preventing reverse flow.

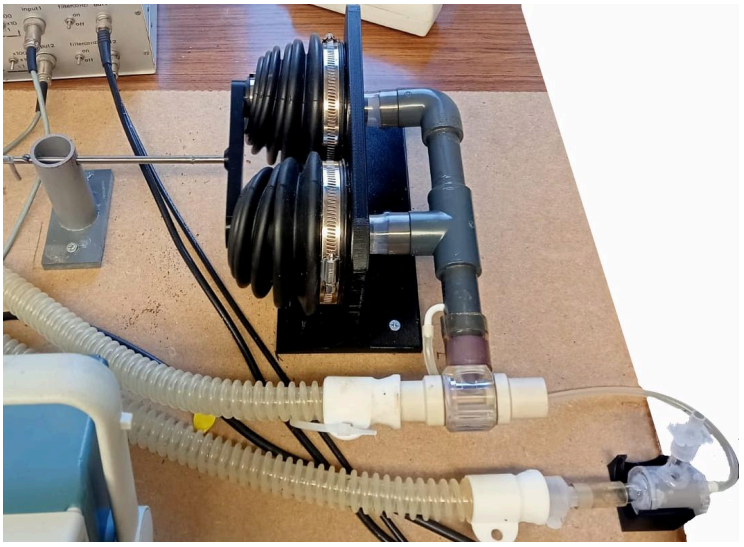

Figure 10. *Valve system during the compression phase. The air is pushed toward the patient circuit as the bellows are compressed. After delivery, the expiratory valve opens to release the used air, followed by the inspiratory valve, which refills the bellows with fresh ambient air during the expansion phase.*

Under regular operation, each valve remains closed unless the corresponding pressure condition is met, thereby minimizing passive leakage and ensuring directional flow.

5.5 Parameter Control and Adjustment

The mechanical ventilator must enable flexible adjustment of key respiratory parameters, primarily breathing frequency and tidal volume, to accommodate a range of patient profiles and clinical scenarios.

5.5.1 Volume Setting

Tidal volume adjustment is achieved mechanically through a variable-stroke mechanism. A stainless steel plate with multiple radial holes is mounted to the motor's output shaft. The attachment point of the linearization linkage can be shifted between these holes, thereby altering the stroke amplitude transmitted to the bellows.

Holes closer to the rotational axis produce smaller displacements and lower delivered volumes.

Conversely, anchoring farther from the center results in larger strokes and increased tidal volumes. However, greater stroke amplitudes induce higher lateral forces within the linearization mechanism, increasing friction and mechanical stress. The mechanical design considered this trade-off, and the plate was dimensioned to ensure an adequate volume adjustment range without compromising system stability.

5.5.2 Frequency Regulation

In this prototype, no pulse-width modulation (PWM) was used. Instead, a regulated voltage source was used to vary the input voltage manually. This allowed for real-time, continuous adjustment of the motor's rotational speed, and thus the breathing frequency, by directly tuning the supply voltage.

Reducing the input voltage results in a lower motor speed, which decreases the breathing frequency. However, lower voltages also reduce the available torque, limiting the system's ability to compress stiffer bellows or effectively overcome higher airway resistance. Conversely, increasing the input voltage raises both the motor speed and torque and elevates the risk of thermal stress and mechanical degradation.

For the adult version of the ventilator, the target frequency range was set at 12 and 24 breaths per minute (bpm), corresponding to motor oscillation frequencies of 200 Hz and 400 Hz, respectively. This range aligns with the normal resting respiratory rate of healthy adults, which typically spans from 12 to 20 breaths per minute, reaching higher values in critical situations [69].

5.5.3 Pressure Monitoring

Pressure must be monitored continuously during mechanical ventilation. This aims to quantify the magnitude of mechanical ventilation, which is particularly evident in pressure-controlled ventilation mode, and to prevent internal injuries caused by over-pressure. In current ventilators, modern electronic sensors track ventilator pressure. However, to follow the project's objective of building an extremely simple ventilator for emergencies in LMICs, a U manometer has been manufactured to avoid using electronic components.

The U-tube manometer is a well-established system for measuring pressure, as it is mechanically simple, accurate, and reliable.

It consists of two vertical tubes linked by a tube forming a U-shaped connection. A differential pressure applied to the tube outlets creates a displacement of the liquid proportional to the pressure. For simplicity, water was used as the liquid, and the tubes were made of glass with a radius of 4.67 mm and an effective liquid column height of 42 cm.

The dynamics of the U-tube are determined by the mechanical balance between a conservative component (liquid mass movement) and a dissipative component (liquid viscosity). The differential equation driving the U manometer [70] is that of a second-order system:

$$\ddot{y}(t) + 2\zeta\omega_n y'(t) + \omega^2{}_n y(t) = \omega^2{}_n u(t) \quad (3)$$

where:

- y: height of the liquid surfaces in the U-tube.
- u(t): input pressure.
- ζ: damping ratio.
- ω_n: natural frequency

From the theoretical model [70], it is demonstrated that

$$\zeta = 2.45\mu\frac{\sqrt{gL}}{R^2\gamma} \quad (4)$$

Thus, ζ depends on liquid viscosity (μ) and specific weight (γ), the length of the total liquid column (L), and the tube radius (R). Moreover,

$$\omega_n = \sqrt{\frac{3g}{2L}} \quad (5)$$

Figure 11 shows the amplitude of the system's frequency response (1). Depending on the ζ value, the system is underdamped ($\zeta < 1$), overdamped ($\zeta > 1$), or critically damped ($\zeta = 1$). Hence, the extent to which the U-tube is suitable for measuring dynamic pressure changes accurately requires a fine design.

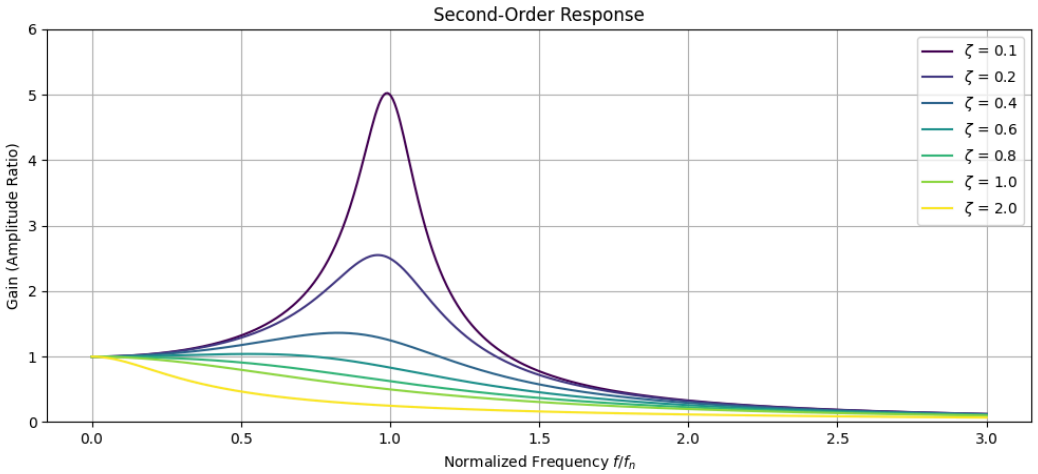

Figure 11. *Frequency response curves for different damping ratios of a second-order instrument.*

For our specific application, where pressures up to 40 cmH_2O must be measured, a suitable total length of water liquid level is L = 0.42 m, resulting in a natural frequency of the U-tube system.

$$\omega_n = \sqrt{\frac{3 \cdot 9.81}{2 \cdot 0.42}} = 6.07\ rad/s = 0.97\ \text{Hz} = 58\ \text{cycles /min}$$

This resonance frequency is close to the breathing frequencies of mechanical ventilation (12-24 cycles/min in adults and up to 45 cycles/min in infants). Therefore, accurate pressure measurement at ventilation frequencies requires that the second-order system has a ζ close to 0.6. In that case, the frequency response would be as shown in Figure 12, indicating the gain amplitude would be close to one for the ventilation frequencies, with errors of only 0.1%, 0.4%, and 2.5% for 12, 24, and 45 resp/min, respectively.

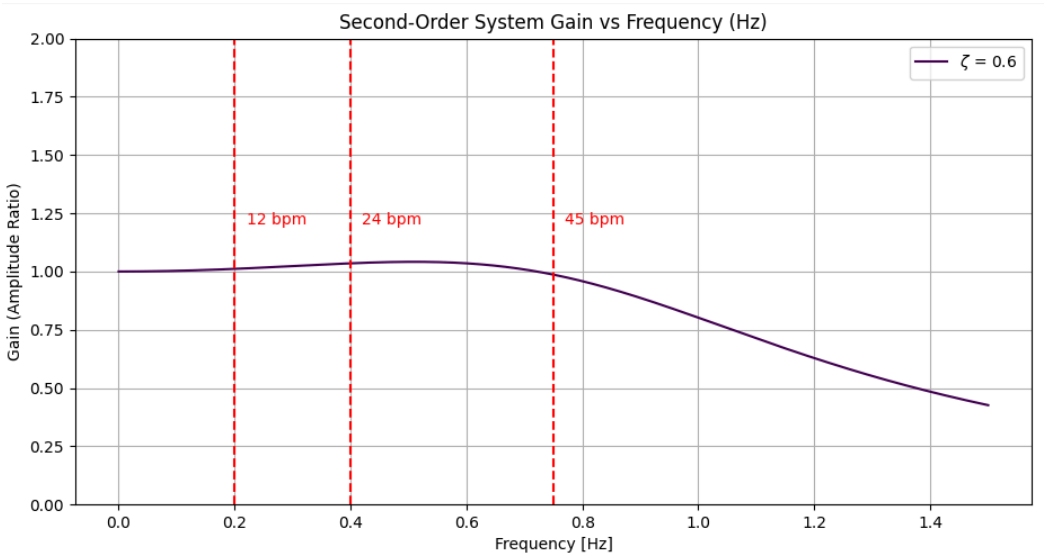

Figure 12. *Gain (amplitude ratio) of a second-order system for damping ratios ζ = 0.6 as a function of frequency (0–1.5 Hz). Vertical dashed lines indicate typical respiratory frequencies for a healthy adult (12 bpm, 0.2 Hz), a patient (24 bpm, 0.4 Hz), and a newborn (45 bpm, 0.75 Hz).*

Theoretically, ζ the U-tube can be determined by setting the tube radius R. From the previous equation, it is shown that for ζ = 0.6, R should be 3.45 mm. Although having a tube with such a radius could be possible, its practical application is not feasible.

Indeed, given the water surface tension effects (which are neglected when modeling the U-tube as a second-order system), moving the water column in such a narrow tube would induce air bubbles, making the U-tube setting unable to measure pressure adequately. An alternative way to reduce ζ with the same tube R is to include an orifice resistance at the collapsible part of the tube at the bottom of the U-tube.

Different strategies were evaluated to regulate the damping of the U-shaped manometer. The most effective solution, meeting all functional requirements while offering smooth, progressive, and continuous adjustment, was using a drip flow controller commonly found in hospital IV systems. This device features a rotating wheel that mechanically compresses the flexible tubing, allowing precise control over fluid resistance. By partially constricting the tube, as shown in Figure 13, the damping behavior of the manometer can be finely tuned.

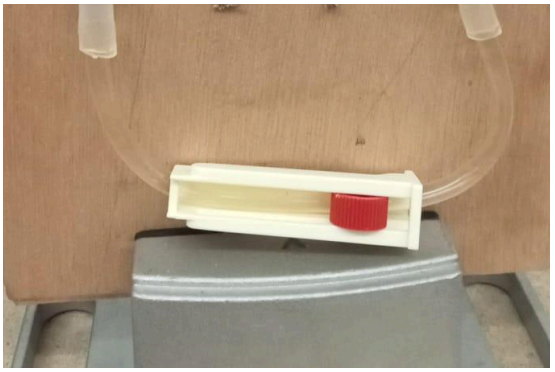

Figure 13. *Drip flow controller integrated into the bottom section of the U-shaped manometer. The wheel mechanism compresses the flexible tubing to adjust flow resistance, allowing fine control of the damping ratio. In this configuration, the tube is set to a low-compression (lightly obstructed) position.*

Therefore, in practice, the U-tube system needs to be adjusted to avoid an overly oscillatory response, where the liquid resonates at a given frequency before stabilizing at the desired value (underdamped), and a sluggish response, where the viscous forces are so strong that it takes a significant amount of time before reaching the desired height (overdamping).

Setting a target of around 0.6 can be easily achieved by following a procedure that does not require an electronic pressure sensor. The U-tube is simply subjected to a (negative) step (e.g., from 20 cmH_2O to zero), and the response is video recorded, e.g., with a smartphone. Frame-to-frame observation of the video enables us to identify several characteristic points, including the maximum and minimum heights of the step response oscillations and their corresponding times. The procedure is repeated by progressively increasing the obstruction (which would progressively dampen the system), as shown in Figure 14:

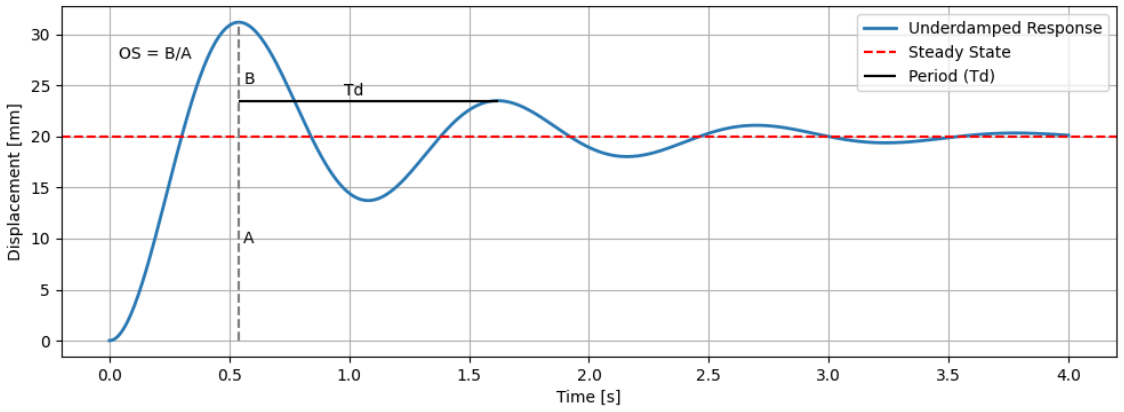

Figure 14. *Theoretical underdamped step response with the overshoot (OS) and the period between oscillations (Td) marked. This response corresponds to the case with no added obstruction in the U-tube system.*

From each step response, we can determine the following parameters:

• Td: Period between oscillations

• OS: Overshoot

According to the system's equation, the damping ratio and the natural and damped frequencies can be calculated from these experimentally measured parameters:

$$\zeta = \frac{-ln(OS)}{\sqrt{\pi^2 + ln(OS)^2}} \quad (6)$$

$$\omega_d = \frac{2\pi}{Td} \quad (7)$$

$$\omega_n = \frac{\omega d}{\sqrt{1-\zeta^2}} \quad (8)$$

The results found in practice by progressively increasing the obstruction are summarized as follows in Figure 15 and Table 2 :

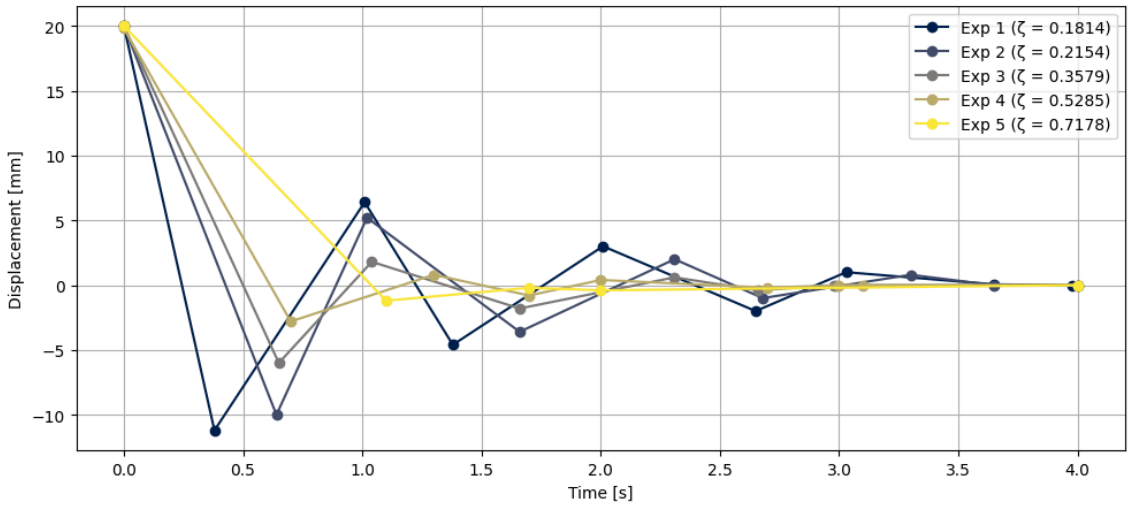

Figure 15. *Experimental step responses of the manometer for increasing levels of obstruction, resulting in different damping ratios (ζ). As obstruction increases, the system transitions from underdamped oscillations to near-critical damping.*

Experiment	ζ	ωd [rad/s]	ωn [rad/s]
1 (no obstruction)	0.1814	5.99	6.088
2	0.2154	5.97	6.12
3	0.3579	6.30	6.74
4	0.5285	6.28	7.40
5	0.7178	4.83	6.94

Table 2. *Damping ratios (ζ), damped natural frequencies (ωd), and undamped natural frequencies (ω_n) for different experimental conditions.*

As mentioned, the desired damping ratio is around 0.6, which is achieved with the last values. When observing the water column, a slight rebound is observed before attaining a stable value after the water column has dropped. The damping ratio achieves the desired values when it minimally decreases just below the steady point and increases until it reaches an optical resolution.

The obstruction solution to increase fluid resistance reduced the damping as expected, but an additional consideration was needed. All theoretical equations assumed linear behavior, but the introduction of obstructions, especially turbulent flow, particularly during the high-speed phases (first oscillation), could affect the system. Minor changes are expected [71], which will slightly increase the damping frequency and coefficient. To confirm that nonlinear effects are negligible in our U-tube manometer, we observed that the effective damping coefficient remained almost constant for different step pressure amplitudes (from 40 cmH_2O to 10 cmH_2O), as shown in Figure 16):

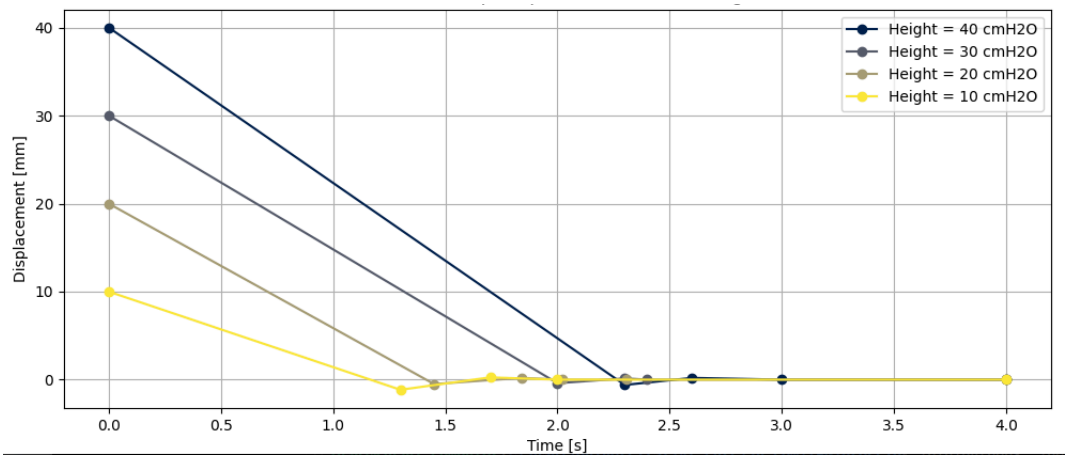

Figure 16. *Manometer step responses for different initial step heights, keeping the obstruction constant. All responses exhibit similar dynamic behavior (damping ratio near critical), confirming that system damping is independent of initial amplitude.*

These data illustrate the potential effectiveness of the U manometer as an easily manufactured pressure monitor in the dynamic range of mechanical ventilation. Although calibration is necessary to ensure a correct response, it can be performed visually by adjusting the step response until a slight rebound (indicating near-critical damping) is achieved. Once tuned, it can accurately reflect rapid pressure changes within the relevant physiological frequency range, as shown later.

To assess the accuracy of the manufactured U-shaped manometer, its readings were compared against those of an electronic pressure transducer across a range of respiratory frequencies with a damping ratio tuned at approximately $\zeta = 0.67$ (video of the step response for this damping ratio), providing a balance between responsiveness and overshoot control. As shown in Figure 17, the pressure readings from the U manometer (Pp(U)) closely match those from the sensor (Pp(Sensor)) at 24 bpm and 12 bpm, with minimal deviation from the electronic transducer values. At these frequencies, the manometer responds reliably and can be considered accurate for practical monitoring.

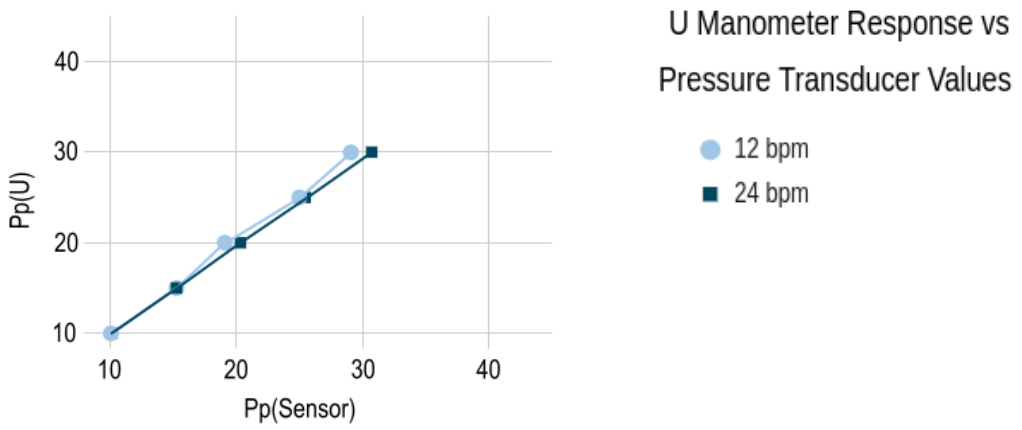

Figure 17. *Comparison between peak pressure values measured by the manufactured U-shaped manometer (Pp(U)) and an electronic pressure transducer (Pp(Sensor)) at two different ventilation frequencies: 12 bpm and 24 bpm.*

However, a clear divergence appears at higher frequencies (specifically 45 bpm), as seen in Figure 18, indicating that the manometer underestimates the peak pressures. This performance difference at high frequencies is consistent with the expected dynamic limitations. These results confirm that the U manometer is suitable for typical adult and low-frequency pediatric applications. However, its use at very high respiratory rates is limited due to dynamic lag.

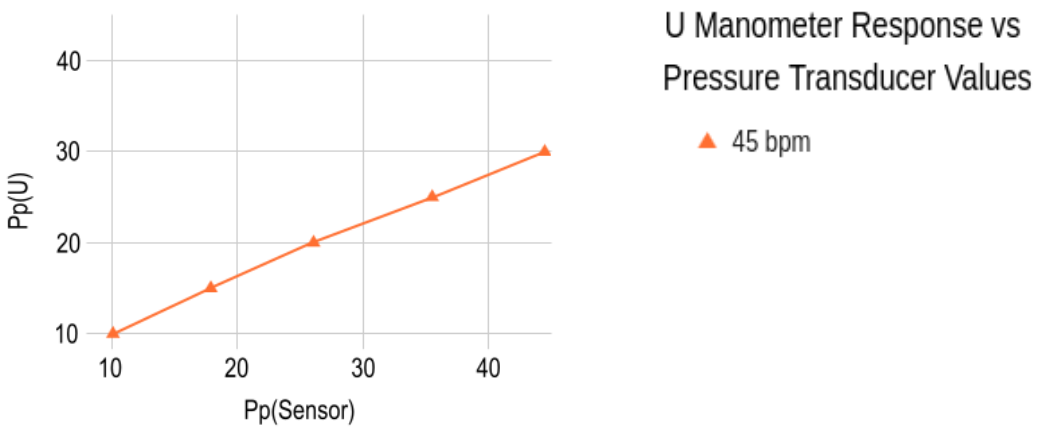

Figure 18. *Comparison between peak pressure values measured by the manufactured U-shaped manometer (Pp(U)) and an electronic pressure transducer (Pp(Sensor)) at 45 bpm.*

It is interesting to note that temperature may considerably modify water viscosity (linear flow energy dissipation) but not density (turbulent energy dissipation).

Temp. °C	Density ρ, kg/m³	Viscosity μ, μPa s from [5]
10	999. 7281	1306. 9
15	999. 1286	1138. 2
20	998. 2336	1002. 0
25	997. 0751	890. 3
30	995. 6783	797. 5
35	994. 0635	719. 5
40	992. 2473	653. 5
45	990. 24	596. 3

Table 3. *Density (ρ) and dynamic viscosity (μ) of water at various temperatures [72].*

Accordingly, depending on the room temperature where the ventilator is placed, the level of obstruction required to achieve almost critical damping may vary. However, this would be minor, as the obstruction mainly dampens the system. Indeed, dissipation in a turbulent-regime obstruction depends on liquid density, not viscosity [71]. As the U-tube damping factor is primarily due to the obstruction, temperature influence is expected to be negligible. Anyway, the degree of obstruction is adjusted at room temperature, where the ventilator is placed.

Furthermore, it is worth noting that, in addition to measuring pressure, the U-tube also serves as a safety valve. Indeed, in case of excessive ventilation pressure, the water in the U-tube is expelled from the open side, releasing excess air pressure and protecting the patient.

5.6 Resistance and Compliance Simulation

To assess the ventilator's performance under different physiological conditions, a series of tests were conducted using a standardized artificial lung model (SmartLung Adult from IMT Analytics) to evaluate the system's adaptability to different respiratory conditions. The artificial lung enables controlled adjustments of compliance and airway resistance, simulating various clinical scenarios.

Adjusting the inflation area of the artificial lung, which represents changes in lung elasticity, modified compliance. At the same time, modifying the diameter of the air entry path varied airway resistance.

Two configurations were primarily evaluated:

- **Healthy lung model:** characterized by low resistance and high compliance, corresponding to standard pulmonary mechanics. The values set were 5 $cmH_2O \cdot s/L$ resistance and 30 mL/cmH_2O compliance.
- **Obstructed-restricted lung model:** featuring increased airway resistance and reduced compliance, simulating patients with obstructive or restrictive pulmonary diseases. The values set were a resistance of 20 $cmH_2O \cdot s/L$ and a compliance of 15 mL/cmH_2O.

Figure 19. *Artificial lung used during testing configured for a healthy configuration.*

These tests validated the ventilator's ability to maintain effective operation across various pathological conditions, verifying that sufficient pressure and volume could be generated even under unfavorable mechanical loads.

5.7 Measurements and Validation

Measurements focused on the system's ability to deliver appropriate tidal volumes under varying mechanical conditions and to operate efficiently and reliably over time.

5.7.1 Volume Measurements

To assess the influence of mechanical configuration on tidal volume delivery, multiple attachment points on the steel plate were tested. Each attachment point corresponded to a different

amplitude of motion, thereby varying the deformation of the bellows and, consequently, the delivered volume.

A comprehensive test was performed by sweeping across amplitude settings under different frequencies and simulated patient conditions. The airflow signal was recorded using a Fleisch pneumotachograph and numerically integrated over time to obtain the delivered volume:

$$V = \int Q(t)dt \tag{9}$$

where:

- V is the delivered volume.
- Q(t) is the flow rate over time.

This resulted in a volume-time curve exhibiting a periodic oscillatory behavior corresponding to the respiratory cycles. The maximum delivered volume for each configuration was determined by measuring the difference between the peak and trough values of the volume curve.

As shown in Figure 20, the ventilator successfully produced distinct volume profiles under two contrasting simulated patient conditions.

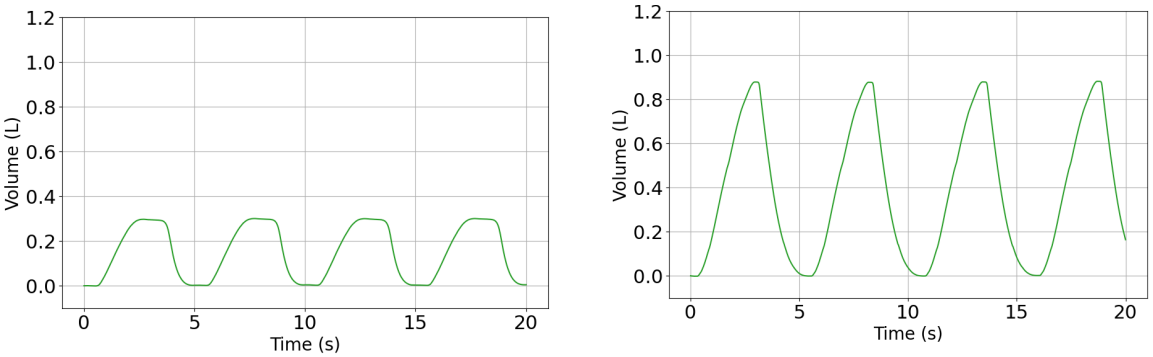

Figure 20. *Representative volume-time curves for two contrasting patient profiles:*
A) 12 breaths per minute (bpm), C = 30 mL/cmH₂O, R = 5 cmH₂O·s/L with low volume delivery.
B) 24 breaths per minute (bpm), C = 15 mL/cmH₂O, R = 20 cmH₂O·s/L with high volume delivery.

Volume measurements confirmed that the ventilator delivers the targeted tidal volume across clinical and mechanical conditions. In Figure 20, the maximum volumes are observed for each amplitude, indicating that the system achieved a delivered volume of approximately 0.7 L without requiring the maximum amplitude setting, thereby meeting the design objective for adult

ventilation. Figure 21 exhibits a near-linear behavior between amplitude and volume, which demonstrates a linear deformation from the CV bellows, and it expected the continuity of this linearity for higher amplitudes, surpassing the 0.8 L target. It should be noted that measurements were limited by the artificial lung used in validation, which had a maximum capacity of 0.6 L, constraining the upper end of the test range.

This data shows the system's performance is predominantly amplitude-governed, with curves for low and high-frequency settings overlapping, indicating minimal dependency on breathing rate. Importantly, even under obstructive/restrictive patient simulations, where elevated compliance and resistance increased the mechanical workload and inner system pressure, the system maintained its ability to deliver clinically relevant volumes. However, a slight difference persisted compared to the healthy model.

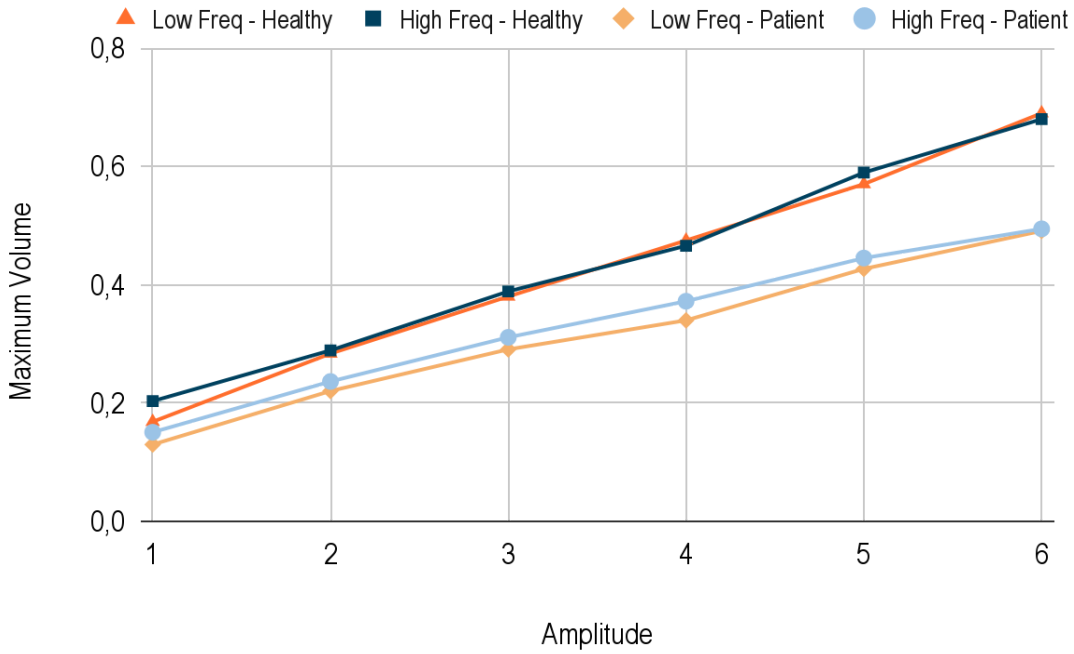

Figure 21. *Maximum delivered volume across amplitude settings. Comparison between healthy and obstructive patient simulations under low- and high-frequency conditions. Post-correction, the system demonstrates an improved, near-linear volume-amplitude relationship with minimal dependence on frequency.*

These final results validate that the ventilator meets its primary functional objectives. However, it is crucial to consider the system improvements implemented during development, which significantly impacted these outcomes.

Early experiments revealed two main issues: limited performance and an inadequate power supply under high-load conditions. As amplitude and obstruction increased, the mechanical load on the motor rose, elevating current demands beyond the capacity of the initial supply and restricting maximum volume delivery. This was resolved by upgrading to a higher-capacity power source.

Second, significant air leakages were detected in the system. Limiting the maximum tidal volume, especially for those cases that generated the highest pressure, as observed in Figure 22. Pressure retention tests, performed by sealing all outlets and observing the pressure decay over time, confirmed the presence of substantial leaks. Soapy water was applied at all junctions and components to identify and localize leakage points, revealing air bubbling from the 3D-printed parts. Despite being printed at 100% infill density, these components exhibited micro-porosity inherent to printing processes.

To address this, all critical 3D-printed components were coated with varnish, forming a hermetic seal. Post-treatment tests showed a marked improvement in pressure retention and volume delivery, confirming the effectiveness of the sealing approach.

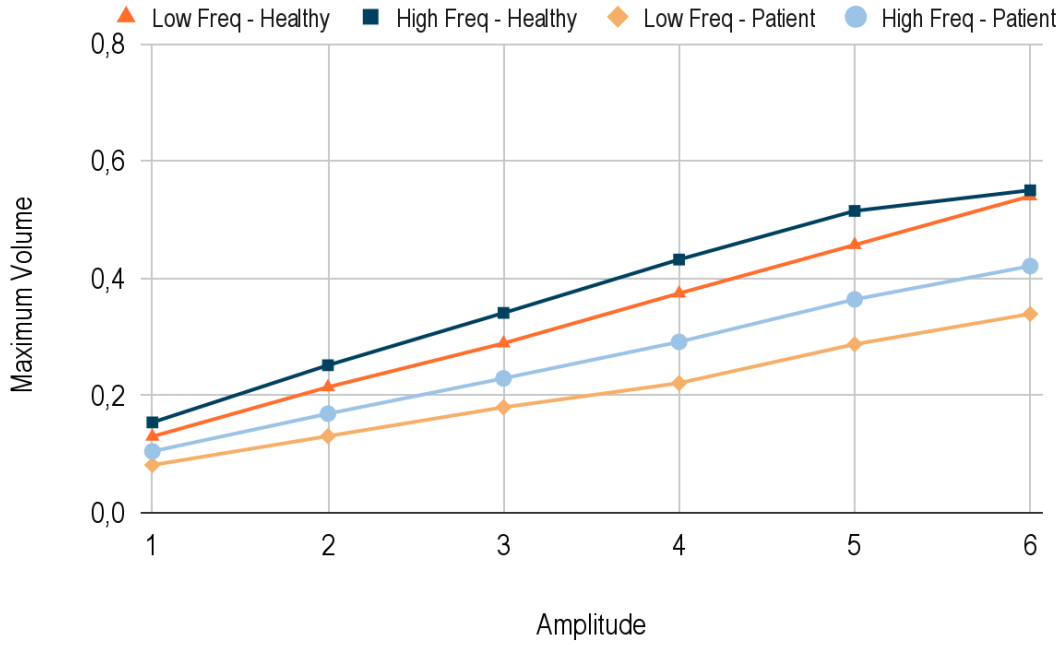

Figure 22. *Maximum delivered volume across amplitude settings before leakage correction. Comparison between healthy and obstructive patient simulations under low- and high-frequency conditions. The data highlight the nonlinear behavior caused by early system limitations, including motor load saturation and air leakage.*

5.7.2 Power Consumption Estimation

To evaluate the power requirements of the ventilator, a low-resistance shunt resistor was connected in series with the motor circuit. By measuring the voltage drop across this resistor, the instantaneous current draw during operation was calculated. This simple yet effective method enables real-time monitoring of energy consumption using basic electrical tools.

The total power consumption recorded over a 10-second test period under normal conditions was 0.0034 Ah, which corresponds to an estimated long-term consumption rate of 1.22 Ah per hour.

This measurement is especially relevant for future versions of the device, which are intended to operate autonomously, such as in field conditions where a connection to the power grid may not be possible. A standard 12V car battery with a capacity of 60 Ah, the most typical size used in medium-sized passenger vehicles, can be used to power the ventilator. Based on the measured consumption, such a battery would be able to operate the system for approximately:

$$\frac{60\ Ah}{1.22\ Ah/h} = 49.2\ hours$$

This estimation demonstrates the ventilator's potential for extended off-grid use, making it a suitable option for unstable or emergency environments where electricity may be intermittent or unavailable.

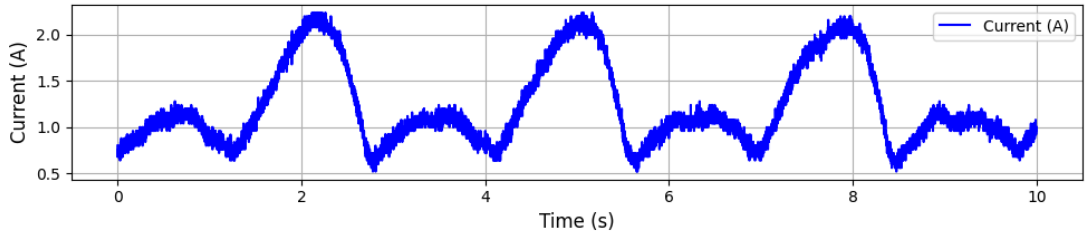

Figure 23. *Current draw (in Amperes) over a 10-second interval during continuous operation.*

5.8 Prototype Enclosure

To improve usability, safety, and transportability, the ventilator prototype was enclosed within a custom wooden support structure equipped with wheels.

The structure was designed to position the ventilator's output port at approximately standard bed height. This positioning enables a straightforward connection to the patient's breathing circuit. Additionally, on one side, it features a cut-out section that provides easy manual access to the stroke adjustment mechanism, allowing for quick changes to the tidal volume without requiring the system to be disassembled.

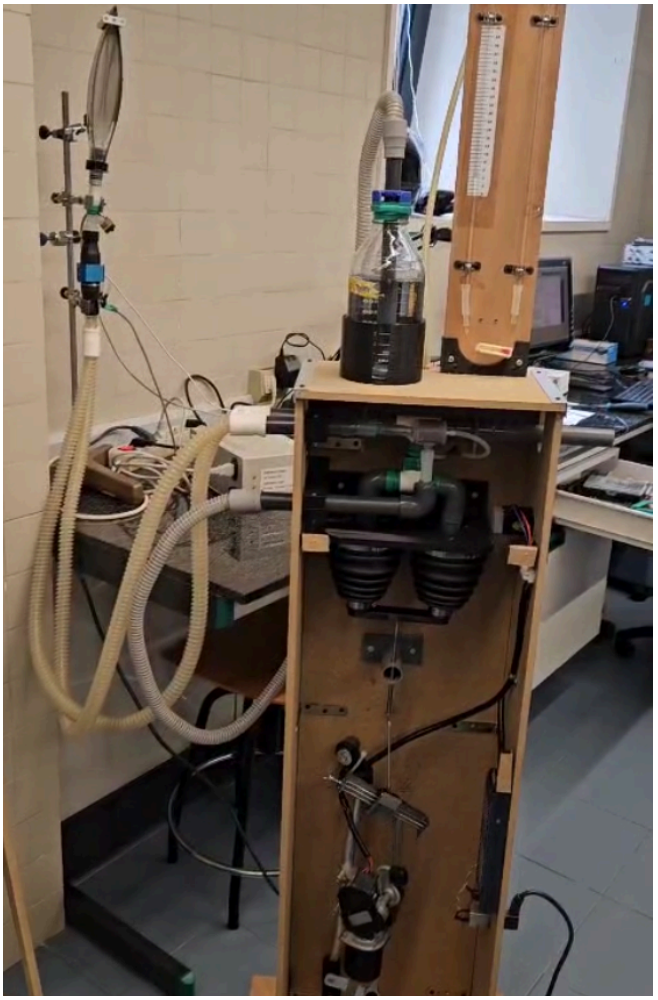

Figure 24. *Full prototype setup during validation testing. The ventilator unit is housed in the mobile wooden enclosure. On the backgroung, the oscilloscope, and artificial lung used for test measurements. Mounted above is the U-shaped manometer.*

5.9 Neonatal Ventilator Adaptation

The ventilator was adapted for neonatal applications to meet the specific requirements of newborn and small infants. The following parameters were used during testing: a resistance of 30 $cmH_2O \cdot s/L$, compliance of 5 mL/cmH_2O, and a frequency of 45 rpm. Based on reference values from the literature [73], the recommended tidal volumes range from 4–6 mL/kg for neonates and 7–10 mL/kg for infants. Experimental measurements showed the system delivered tidal volumes from 18.8 mL (at the lowest amplitude setting) to 118.1 mL (at the highest setting) per breath. Using the relation:

$$W_{MAX}(kg) = \frac{V_{MESURED}(mL)}{V_{RECOMMENDED}(mL/kg)} \quad (10)$$

where:

- W_{MAX}: maximum body weight. (kg)
- $V_{MESURED}$: measured tidal volume. (mL)
- $V_{RECOMMENDED}$: recommended tidal volume per kg. (mL/kg)

The equation determines that this range covers neonates with body weights from approximately 3 kg (minimum) up to larger infants around 12–16 kg, depending on the amplitude setting. As shown in Figure 25, the system achieves this by delivering tidal volumes between 20 mL and 120 mL per breath, which corresponds to the minimum and maximum amplitude settings, respectively.

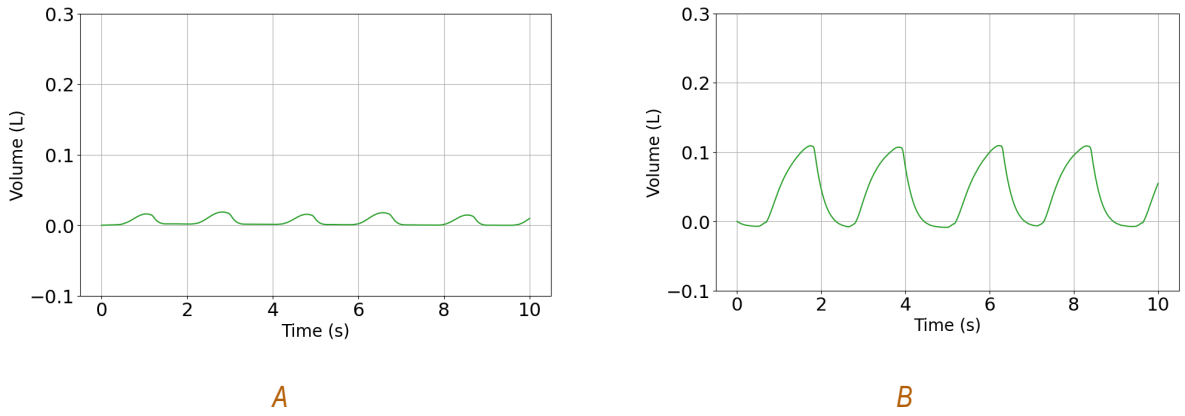

Figure 25. *Representative volume-time curves obtained with the neonatal mechanical ventilator at a frequency of 35 breaths per minute (bpm), with compliance of 10 mL/cmH₂O and resistance 50 cmH₂O·s/L.*
A) Minimum volume setting.
B) Maximum volume setting.

The relationship between amplitude settings and delivered tidal volume was further characterized by plotting the maximum volume against each amplitude level. As shown in Figure 26, the ventilator demonstrates a progressive increase in delivered volume across the range of amplitude settings. This linear-like behavior confirms that the system can be finely adjusted to suit various neonatal and infant weight categories, maintaining precision even at low volumes.

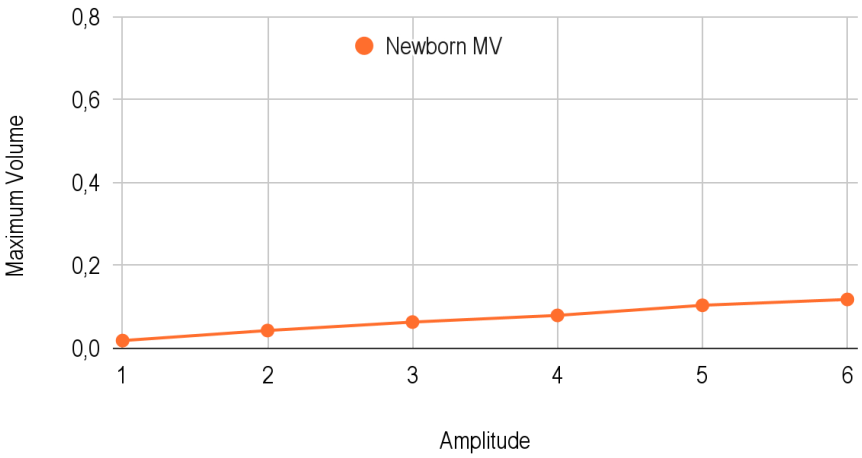

Figure 26. *Maximum delivered volume across amplitude settings for the neonatal ventilator.*

These results confirm the system's suitability for full-term neonates, potentially extending into early pediatric applications.

A key difference between the adult and neonatal versions is that the neonatal system utilizes a smaller rear motor designed for occasional, non-continuous use. During testing, the motor experienced overheating at higher frequencies, which was resolved by installing a standard computer fan for active cooling. Additionally, the neonatal ventilator incorporates more small bellows to precisely deliver low tidal volumes at the required high respiratory rates. These adaptations, combined with the selected compliance and resistance settings, ensured the device could ventilate neonates and infants safely and effectively within the established target range.

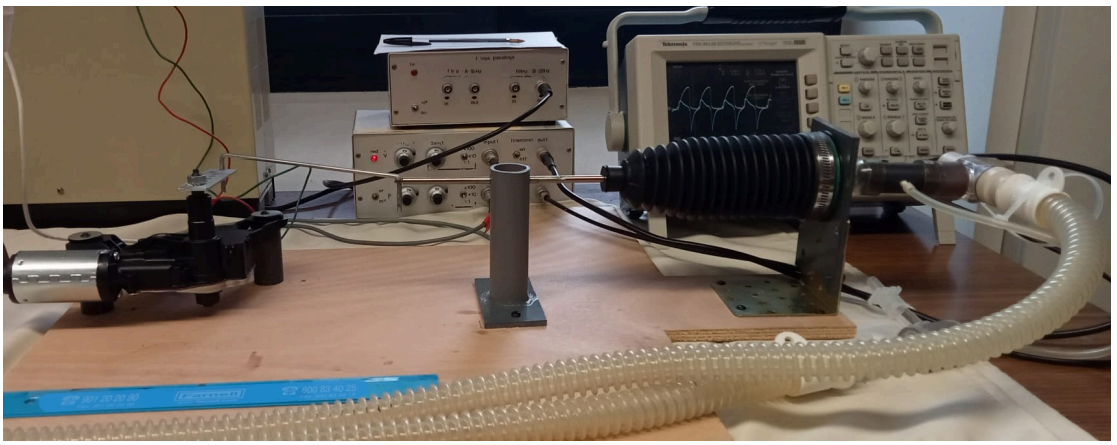

Figure 27. *Experimental setup of the compact mechanical ventilator designed for newborns. The background shows the signal acquisition system, including amplifiers and an oscilloscope that monitors the pneumotachograph and pressure transducer outputs in real-time.*

6 EXECUTION TIMING

This section outlines the action plan for developing the described project, including its work sequence, schedule, and resource allocation. For this, tools such as Work Breakdown Structure (WBS), Gantt chart, and task tracking are used to schedule and monitor progress throughout the project. These aids enabled verification that critical stages, such as design, prototyping, testing, and documentation, were executed in a harmonized and prompt manner, thereby improving efficiency as well as project viability.

The development of this project was initiated through an internship, during which the initial research, conceptualization process, and first sketches began. The project was then resumed and worked on during the 2024–2025 academic year as part of the Final Degree Project.

6.1 Milestone Plan

The milestone plan outlines the key phases and deliverables that structured the execution of the ventilator development. Each milestone marks the completion of a critical component or stage, ensuring that the project advanced in a systematic and organized manner. The following milestones were defined:

Milestone	Description	Date
M1 – Project Definition	Initial research, problem definition, and project scoping during the internship	July 2024
M2 – Background and Literature Review	Collection and analysis of prior work, physiological principles, and market data	September 2024
M3 – Conceptual Design	Identification of requirements, component selection, and early sketches	October 2024
M4 – Prototype Development	Assembly of core subsystems and initial adult prototype configuration	November 2024
M5 – Functional Testing	Benchtesting of the adult prototype under simulated respiratory conditions	December - January 2024
M6 – Neonatal Version Development	Adaptation of design for neonatal use, testing at higher frequencies	February 2025
M7 – Parameter Validation	Performance measurements: tidal volume, pressure, and compliance simulation	March 2025

M8 – Final Improvements and Enclosure	Sealing, structural refinement, and housing design	April 2025
M9 – Report Writing and Review	Documentation, result analysis, and thesis preparation	May 2025
M10 – Project Submission	Final submission of the thesis and supplementary materials	June 2025

Table 4. *Project milestone plan outlining the key phases of development. Each milestone represents a major project checkpoint tied to specific deliverables and timeframes.*

6.2 WBS Diagram

This Work Breakdown Structure (WBS) diagram captures the project's structure, starting from high-level work packages and drilling down to detailed tasks. This hierarchical approach ensures that all aspects of the project are covered and clearly defined.

The WBS for this project reflects the five primary phases: project planning and management, system design, system development, testing and validation, and final reporting. Each phase is further divided into specific tasks required to achieve the final objective: developing an accessible, low-cost mechanical ventilator.

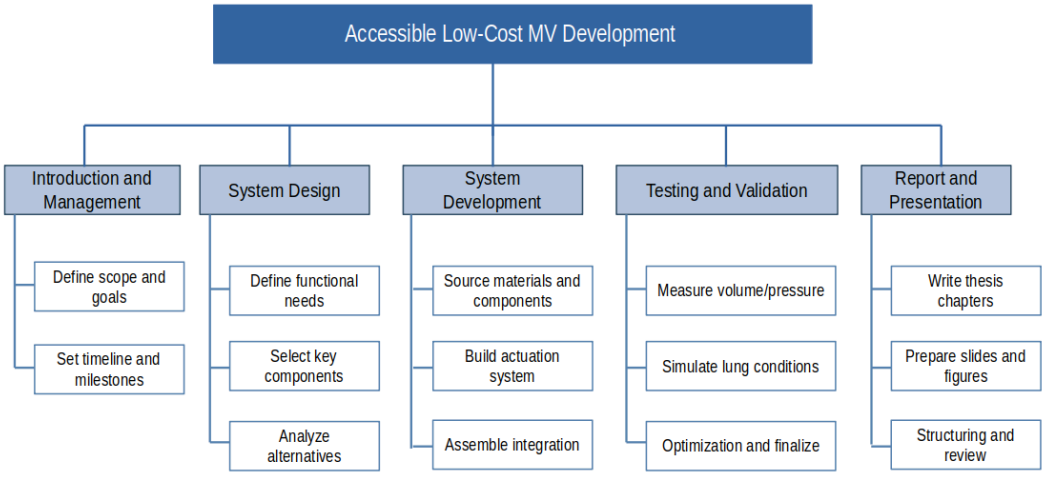

Figure 28. *WBS of the project. The diagram outlines the main project phases and associated tasks, from early planning through design, development, testing, and reporting.*

6.3 WBS Dictionary

The Work Breakdown Structure (WBS) dictionary provides detailed information about each task in the WBS diagram 3. The following tables contain information related to each task, including the work package to which it belongs, the task description, corresponding deliverables, the responsible person, the task approver, the expected completion time, and the assigned resources.

In total, fourteen tasks comprise the project, and these are described in the following tables. Each task is meticulously documented to ensure clarity and accountability. The tables provide a comprehensive overview of all aspects of the project. This structured approach facilitates efficient project management and ensures the successful completion of project objectives.

Work package name	Introduction and management	WBS code	1
Task name	Define scope and goals	Task Code	1.1
Description			
Define project objectives and expected outcomes			
Acceptance Criteria			
Clear, written scope and goal document approved			
Deliverable Description	Scope and goals summary document		
Limit Date	14 Jul 2024	Estimated Duration	2 weeks

Table 5. *Description of task 1.1. Define scope and goals*

Work package name	Introduction and management	WBS code	1
Task name	Set timeline and milestones	Task Code	1.2
Description			
Develop detailed project schedules and milestones			
Acceptance Criteria			
Approved timeline with realistic milestones			
Deliverable Description	Timeline and milestone chart		
Limit Date	21 Jul 2024	Estimated Duration	1 week

Table 6. *Description of task 1.2. Set timeline and milestones*

Work package name	System Design	WBS code	2
Task name	Define functional needs	Task Code	2.1
Description			
Identify clinical and technical requirements			
Acceptance Criteria			
Complete list of prioritized needs			
Deliverable Description	Functional requirements document		
Limit Date	30 Sep 2024	Estimated Duration	2 weeks

Table 7. *Description of task 2.1. Define functional needs*

Work package name	System Design	WBS code	2
Task name	Select key components	Task Code	2.2
Description			
Choose motors, bellows, control parts			
Acceptance Criteria			
Components sourced and technically validated			
Deliverable Description	Selected components list		
Limit Date	20 Oct 2024	Estimated Duration	2.5 weeks

Table 8. *Description of task 2.2. Select key components*

Work package name	System Design	WBS code	2
Task name	Analyze alternatives	Task Code	2.3
Description			
Compare options, weigh pros/cons			
Acceptance Criteria			
Selection rationale documented			
Deliverable Description	Alternatives evaluation report		
Limit Date	31 Oct 2024	Estimated Duration	2 weeks

Table 9*. Description of task 2.3. Analyze alternatives*

Work package name	System Development	WBS code	3
Task name	Source materials/components	Task Code	3.1
Description			
Procure parts and materials			
Acceptance Criteria			
All parts received, checked for defects			
Deliverable Description	Inventory and sourcing record		
Limit Date	21 Nov 2024	Estimated Duration	3 weeks

Table 10. *Description of task 3.1. Source materials/components*

Work package name	System Development	WBS code	3
Task name	Build actuation system	Task Code	3.2
Description			
Assemble motor, linkage, frame			
Acceptance Criteria			
System operates mechanically without major issues			
Deliverable Description	Built actuation assembly		
Limit Date	15 Dec 2024	Estimated Duration	4 weeks

Table 11. *Description of task 3.2. Build actuation system*

Work package name	System Development	WBS code	3
Task name	Assemble integration	Task Code	3.3
Description			
Connect bellows, electronics, sensors			
Acceptance Criteria			
Fully integrated, ready for testing			
Deliverable Description	Assembled ventilator prototype		
Limit Date	31 Dec 2024	Estimated Duration	3 weeks

Table 12. *Description of task 3.3. Assemble integration*

Work package name	Testing and Validation	WBS code	4
Task name	Measure volume/pressure	Task Code	4.1
Description			
Perform performance tests			
Acceptance Criteria			
Volume/pressure test report			
Deliverable Description	Selected components list		
Limit Date	21 Jan 2025	Estimated Duration	3 weeks

Table 13. *Description of task 4.1. Measure volume/pressure*

Work package name	Testing and Validation	WBS code	4
Task name	Simulate lung conditions	Task Code	4.2
Description			
Test on normal and obstructive models			
Acceptance Criteria			
Data collected under both conditions			
Deliverable Description	Simulation report		
Limit Date	5 Feb 2025	Estimated Duration	3 weeks

Table 14. *Description of task 4.2. Simulate lung conditions*

Work package name	Testing and Validation	WBS code	4
Task name	Optimization and finalize	Task Code	4.3
Description			
Refine system, fix issues			
Acceptance Criteria			
Improved performance, documented changes			
Deliverable Description	Optimization and final report		
Limit Date	10 Mar 2025	Estimated Duration	2.5 weeks

Table 15. *Description of task 4.3. Optimization and finalize*

Work package name	Report and Presentation	WBS code	5
Task name	Write thesis chapters	Task Code	5.1
Description			
Draft and edit thesis sections			
Acceptance Criteria			
Complete, edited thesis			
Deliverable Description	Written thesis document		
Limit Date	1 June 2025	Estimated Duration	2.5 weeks

Table 16. *Description of task 5.1. Write thesis chapters*

Work package name	Report and Presentation	WBS code	5
Task name	Prepare slides/figures	Task Code	5.2
Description			
Choose motors, bellows, control parts			
Acceptance Criteria			
Components sourced and technically validated			
Deliverable Description	Selected components list		
Limit Date	31 May 2025	Estimated Duration	2.5 weeks

Table 17. *Description of task 5.2. Prepare slides/figures*

6.4 Preceding Analysis

Table 18 lists each task with its predecessor dependencies, providing a precedence analysis so that all activities proceed in the correct sequence.

Code	Task Name	Predecessors	Comments
1.1	Define scope and goals	—	Starting point
1.2	Set timeline and milestones	1.1	Scheduling depends on the scope
2.1	Define functional needs	1.1, 1.2	Needs both scope and basic scheduling
2.2	Select key components	2.1	Functional needs must be precise before selecting parts
2.3	Analyze alternatives	2.1, 2.2	Based on defined needs and selected components
3.1	Source materials/components	2.2	Can begin as components are selected
3.2	Build actuation system	3.1, 2.3	Requires sourced parts and chosen configuration
3.3	Assemble integration	3.2	Once the actuator is ready
4.1	Measure volume/pressure	3.2, 3.3	Can begin as soon as the system is mechanically sound
4.2	Simulate lung conditions	4.1	Follows baseline measurement tests
4.3	Optimization and finalize	4.2	Final adjustments after simulation
5.1	Write thesis chapters	3.3, 4.2	Writing can begin with the system complete and test data
5.2	Prepare slides/figures	5.1, 4.3	Needs finalized system and written material

Table 18. *Precedence analysis showing task dependencies across project phases.*

6.5 PERT

The following PERT diagram visually represents the logical and temporal sequence of tasks based on the precedence analysis. Each node includes the task duration, as well as the earliest and latest possible start and finish times. The diagram has been instrumental in ensuring a coherent schedule aligned with available resources and the timeline.

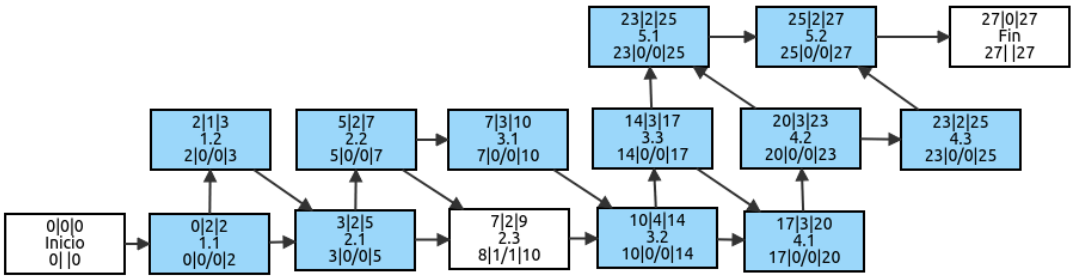

Figure 29. *PERT diagram of the project. Each task is labeled with its duration, earliest and latest start and finish times, and slack. The critical path is composed of tasks with zero slack and defines the shortest possible duration of the project.*

6.6 GANTT

Figure 30 shows the year-long project plan broken into five color-coded phases: planning , design, development, testing/validation, and report/thesis work. Arrows indicate task dependencies, ensuring each stage flows into the next and all major milestones are met on schedule.

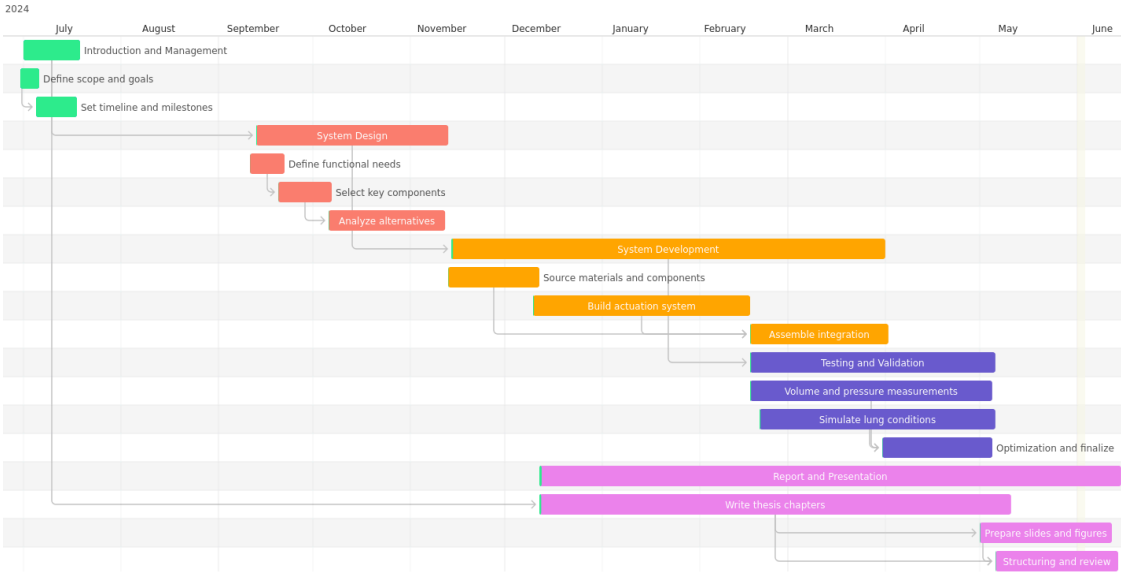

Figure 30. *Project Timeline Gantt Chart (July 2024 – June 2025)*

6.7 Deliverables List

Deliverable Code	Deliverable Name	Description	Task Code
D1	Scope and goals summary document	Written document defining project objectives and intended outcomes	1.1
D2	Timeline and milestone chart	Visual schedule of project phases and checkpoints	1.2
D3	Functional requirements document	Prioritized list of technical and clinical needs	2.1
D4	Selected components list	Validated list of motors, sensors, and control elements	2.2
D5	Alternatives evaluation report	Comparison and justification of design options	2.3
D6	Inventory and sourcing record	Log of materials and components sourced for the prototype	3.1
D7	Built actuation assembly	Mechanically functioning actuation system	3.2
D8	Assembled ventilator prototype	Integrated ventilator system ready for testing	3.3
D9	Volume/Pressure test report	Test data for tidal volume and airway pressure under load	4.1
D10	Simulation report	Results from tests simulating healthy and obstructed lungs	4.2
D11	Optimization and final report	Summary of performance improvements and final design refinements	4.3
D12	Written thesis document	Full academic report of project scope, development, and results	5.1
D13	Presentation slides and figures	Visual materials prepared for thesis defense and final presentation	5.2

Table 19. *List of project deliverables linked to specific WBS tasks. Each deliverable represents a tangible outcome of the project.*

7 TECHNICAL VIABILITY

From a technical standpoint, the proposed ventilator has proven to be a practical and reliable solution, particularly in emergency contexts where conventional medical equipment is unavailable. The core idea of utilizing commonly available automotive components, such as windshield wiper motors and CV joint bellows, has been validated through rigorous testing and careful design iterations.

One of the system's greatest strengths is its simplicity. Its mechanical design can be assembled with basic tools and skills, requiring no advanced infrastructure. Components can be sourced from various vehicles, making the design flexible and adaptable across different regions.

Although some structural and functional components were 3D printed during development mainly to speed up iteration and simplify testing, using a 3D printer is not essential. Depending on local resources, all printed parts can be easily fabricated using commonly available materials such as wood, PVC, rubber, or metal. The design was intentionally kept simple to allow for replication in workshops without access to additive manufacturing technologies.

In terms of performance, the ventilator successfully delivers a wide range of tidal volumes and frequencies, and maintains safe pressure limits across various simulated respiratory conditions. The manometer proved to be an effective and low-cost solution for continuous pressure monitoring. While it does not aim to replace hospital-grade ventilators, the device offers a technically sound alternative for low-resource settings or emergency scenarios where time, cost, and availability are critical factors.

Strengths	**Weaknesses**
• Built from readily available automotive parts, compatible with components from almost any brand. • Easy to assemble, repair, and adapt locally with minimal resources. • Mechanically robust and power-efficient: ideal for unstable or mobile environments.	• Not certified for clinical use; limited to emergency or humanitarian applications. • Manual control of parameters lacks the precision of fully electronic systems. • No assured lifespan or durability rating due to using repurposed, non-medical components.
Opportunities	**Threats**
• Highly scalable through local manufacturing or NGO-led initiatives. • Ideal for rapid response in disaster zones or health crises. • Can be a valuable training or backup tool in low-resource healthcare settings.	• Even basic tools or replacement parts may not be available in some locations, compromising long-term use. • A lack of trained personnel could limit its practical deployment. • Devices deployed in harsh climates could degrade faster than anticipated.

Table 20. *DAFO Analysis: Strengths, Weaknesses, Opportunities, and Threats*

8 ECONOMICAL VIABILITY

The development of this emergency-use mechanical ventilator was guided by a core objective: achieving maximum cost-effectiveness while satisfying critical clinical requirements. Conventional mechanical ventilators often cost upwards of $20,000, a price point that places them out of reach for LMICs, and even poses challenges for high-income nations during times of crisis or shortage.

The proposed design significantly reduces costs by leveraging readily available, low-cost automotive components such as windshield wiper motors, CV joint bellows, and inner tie rod boots. The estimated material cost per adult ventilator unit is approximately US$300–US$500, depending on local market prices, with the neonatal version falling within a similar range.

Key economic advantages include:

- **Low material costs**: Using off-the-shelf components avoids the need for custom-manufactured parts.
  Simple manufacturing: Assembly can be done without specialized machinery or highly skilled labor.
- **Repairability**: Components can be easily replaced using local supply chains, reducing long-term maintenance costs.
- **Scalability**: Designs are adaptable to decentralized, small-batch production, which is crucial in times of crisis.
- **Widespread availability:** Components are commonly used across the global automotive market and are compatible with parts from a wide range of brands, ensuring accessibility even in diverse or remote contexts.

The following tables detail the material costs associated with the final prototype based on components purchased from low-cost online platforms (e.g., Amazon, Alibaba) or already available in the laboratory. Basic supplies, such as silicone, fasteners, and general workshop tools, are not included in the price. Similarly, components that were tested during development but ultimately excluded from the final design have been omitted.

While the listed prices reflect individual, prototype-stage purchases, all selected components are widely available through local automotive suppliers, hardware stores, or surplus sources. In emergency deployments, particularly in LMICs, many of these parts could be salvaged from hospital inventory, used vehicles, or community resources, potentially reducing the material cost to near zero.

Component	Qty	Model Used	Unity Cost	Total Cost
Front windshield wiper motor with linkage	1	CWM15100OS / 8200268931 (Renault Clio III)	80.59 €	80.59 €
CV Joint bellows with stainless steel ear clamps	2	Split silicone CV boot, universal fit	9.69 €	19.38 €
			Total	**109.97 €**

Table 21. *Component cost breakdown for the adult version of the mechanical ventilator prototype.*

Component	Qty	Model Used	Unity Cost	Total Cost
Rear windshield wiper motor	1	A-Premium, 5-pin (Jeep Liberty 2008–2012), 57010090AB/AC	77.99 €	77.99 €
Rack Boot Kit with stainless steel ear clamps	1	Beck Arnley 103-3069 – Steering rack boot kit	12.43 €	12.43 €
Cooling fan	1	Tacens Anima AF8 – 80 mm, 12 V, 1800 RPM, 14 dB, 7 blades	2.19 €	2.19 €
			Total	**92.61 €**

Table 22. *Component cost breakdown for the neonatal version of the mechanical ventilator prototype.*

Component	Qty	Model Used	Unity Cost	Total Cost
Hans Rudolph bidirectional valve	1	Two-Way Non-Rebreathing T-Shape Valve	302,98 €	302,98 €
Roller clamp from the drip chamber	1	Standard Luer-Lock drip chamber	0.31 €	0.31 €
PLA+ filament spool	200 gr	SUNLU PLA Plus, 1.75 mm, black, 1 kg, ±0.02 mm tolerance	-	3.34 €
Swivel caster wheels	1 set (4 pcs)	HOLKIE, 75 mm wheels, M10×1.5 threaded stem	19.99 €	19.99 €
			Total	**326.62 €**

Table 23. *List of components shared across both adult and neonatal ventilator versions.*

Based on the material breakdown, the total cost of the adult prototype is approximately €436.59, while the neonatal version is around €419.23. These values could be significantly reduced in emergency scenarios through the reuse of parts, local sourcing, or bulk purchasing. The design's modularity also allows selective substitution of components without compromising core functionality.

9 LEGAL AND REGULATORY ASPECTS

Mechanical ventilators are categorized as medical equipment and are subject to rigorous regulatory systems to guarantee their safety, efficacy, and quality. Ventilators in the European Union are regulated under the Medical Device Regulation (MDR), which replaced the former Medical Devices Directive 93/42/EEC in May 2021 [74]. This rule outlines the requirements for post-market surveillance, labeling, risk management, technical documentation, clinical evaluation, and device classification [74].

The MDR states that a mechanical ventilator meant for clinical use must undergo extensive conformity assessment processes, including testing for electrical safety, electromagnetic compatibility, biocompatibility, software validation (if relevant), and performance under simulated clinical conditions [75], [76]. Furthermore, the device must get a CE marking before it may be sold on the European market [74].

This initiative emphasizes the European setting, even if comparable regulatory systems exist elsewhere (such as the FDA process in the United States or ANMAT in Argentina) [77].

It should be emphasized that the ventilator created in this project is intended as a last-resort, emergency-use appliance for extreme resource-limited circumstances, such as during a pandemic or catastrophe when commercial ventilators are unavailable. It does not satisfy the MDR or comparable systems' complete certification and regulatory criteria. Intended solely for emergency humanitarian or compasive use, the design would need significantly more development, validation, and licensing in case of intending conventional regulatory approval [78], [79].

This distinction corresponds with several international emergency programs, including the WHO Emergency Use Listing or FDA Emergency Use Authorizations, which have offered temporary regulatory pathways during health emergencies [78]. Using such devices in every circumstance would call for ethical oversight, cooperation with local health authorities, and a risk-benefit analysis [77].

10 CONCLUSIONS AND FUTURE LINES

This project successfully achieved its primary objective: to design, build, and validate low-cost mechanical ventilators utilizing commonly available, non-medical components.

In this case, two models have been developed: one for adults and another for neonatal use. Both devices were tested under simulated clinical conditions and demonstrated the capability to reliably deliver the necessary respiratory support parameters, including adjustable tidal volume and frequency.

Experimental results confirmed that each prototype could generate both the maximum and minimum ventilation volumes required within their respective clinical ranges. The adult system consistently delivered volumes meeting the standard for adult ventilation. Similarly, the neonatal version was able to generate small tidal volumes suitable for newborns with adequate frequency control.

Breathing frequency was effectively regulated in both systems through manual voltage adjustments, and volume was adjusted mechanically via a radial crank mechanism.

Furthermore, the water-based U-tube manometer integrated for pressure monitoring functioned as both a real-time analog indicator and a passive safety valve. It demonstrated reliable performance at standard respiratory rates and helped prevent overpressurization, supporting the system's safety profile.

Importantly, all components used in the final design are widely available from the global automotive and hardware sectors. This includes motors, bellows, valves, clamps, and support materials, which can often be locally sourced or repurposed from used equipment. In LMICs or emergency contexts, this could drastically reduce costs or even bring them close to zero.

Despite these achievements, the project recognizes its limitations, particularly the absence of clinical trials and full regulatory compliance. The ventilators are intended strictly for emergency, last-resort situations in resource-limited environments where conventional equipment is unavailable.

10.1 Future Work

This project continues to evolve, with several improvements already underway. One key area of development is the integration of a battery-powered system, enabling the ventilator to operate in off-grid or unstable power environments. Additionally, the integration of a PWM (Pulse Width Modulation) controller will facilitate precise regulation of motor speed. This will eliminate the need for manual voltage adjustment and improve control over respiratory frequency.

The volume adjustment mechanism is also being redesigned. In the current version, tidal volume changes require the system to be stopped; future iterations aim to allow continuous, real-time volume control during operation, thereby enhancing clinical flexibility and usability.

In terms of validation, preclinical testing is a necessary next step. Controlled trials, using both animal models and then clinical trials with humans, will be essential for assessing the safety and performance of devices under real physiological conditions. It is worth mentioning that a refined version of this ventilator will be tested by late 2025 in a porcine model at the animal facility of the Faculty of Medicine and Health Sciences. This in vivo test has been approved by the *Comitè Ètic d'Experimentació Animal (CEEA)* and will be carried out with the financial support of a SEPAR project *"Ventilador mecánico de bajo coste y construcción simple con descripción en modo abierto: Desarrollo y evaluación en banco de pruebas y en modelo porcino*", in collaboration with members of the Respiratory Intensive Care of the Hospital Clínic.

These ongoing improvements and future evaluations aim to strengthen further the system's functionality, autonomy, and clinical relevance, bringing it closer to a reliable solution for emergency ventilation where it is most critically needed.

11 BIBLIOGRAPHY

[1] K. M. Agarwal, P. Sharma, D. Bhatia, and A. Mishra, "Concept design of the physical structure for ICU ventilators for COVID-19 pandemic," *Sens. Int.*, vol. 2, p. 100092, Jan. 2021, doi: 10.1016/j.sintl.2021.100092.

[2] "Global burden of chronic respiratory diseases and risk factors, 1990–2019: an update from the Global Burden of Disease Study 2019 | Institute for Health Metrics and Evaluation." Accessed: May 31, 2025. [Online]. Available: https://www.healthdata.org/research-analysis/library/global-burden-chronic-respiratory-diseases-and-risk-factors-1990-2019

[3] GBD 2015 Chronic Respiratory Disease Collaborators, "Global, regional, and national deaths, prevalence, disability-adjusted life years, and years lived with disability for chronic obstructive pulmonary disease and asthma, 1990-2015: a systematic analysis for the Global Burden of Disease Study 2015," *Lancet Respir. Med.*, vol. 5, no. 9, pp. 691–706, Sep. 2017, doi: 10.1016/S2213-2600(17)30293-X.

[4] C. Torres-Duque, D. Maldonado, R. Pérez-Padilla, M. Ezzati, and G. Viegi, "Biomass Fuels and Respiratory Diseases," *Proc. Am. Thorac. Soc.*, vol. 5, no. 5, pp. 577–590, Jul. 2008, doi: 10.1513/pats.200707-100RP.

[5] A. M. Al Husseini *et al.*, "Design and Prototyping of a Low-Cost Portable Mechanical Ventilator," *J. Med. Devices*, vol. 4, no. 027514, Aug. 2010, doi: 10.1115/1.3442790.

[6] M. L. Ranney, V. Griffeth, and A. K. Jha, "Critical Supply Shortages - The Need for Ventilators and Personal Protective Equipment during the Covid-19 Pandemic," *N. Engl. J. Med.*, vol. 382, no. 18, p. e41, Apr. 2020, doi: 10.1056/NEJMp2006141.

[7] N. Dube, Q. Li, K. Selviaridis, and M. Jahre, "One crisis, different paths to supply resilience: The case of ventilator procurement for the COVID-19 pandemic," *J. Purch. Supply Manag.*, vol. 28, no. 5, p. 100773, Dec. 2022, doi: 10.1016/j.pursup.2022.100773.

[8] S. Oberloier, N. Gallup, and J. M. Pearce, "Overcoming supply disruptions during pandemics by utilizing found hardware for open source gentle ventilation," *HardwareX*, vol. 11, p. e00255, Apr. 2022, doi: 10.1016/j.ohx.2021.e00255.

[9] A. Abba *et al.*, "The novel Mechanical Ventilator Milano for the COVID-19 pandemic," *Phys. Fluids Woodbury N 1994*, vol. 33, no. 3, p. 037122, Mar. 2021, doi: 10.1063/5.0044445.

[10] J. M. Pearce, "A review of open source ventilators for COVID-19 and future pandemics," *F1000Research*, vol. 9, p. 218, Apr. 2020, doi: 10.12688/f1000research.22942.2.

[11] F. Fox, J. Hayes, B. Whelan, D. Casey, and M. Connolly, "Key Factors Impacting a Medical Ventilator Supply Chain During the COVID- 19 Pandemic: Lessons for Pandemic Preparedness," *Disaster Med. Public Health Prep.*, vol. 18, p. e65, Jan. 2024, doi: 10.1017/dmp.2024.55.

[12] C. Carter, N. Thi Lan Anh, and J. Notter, "COVID-19 disease: perspectives in low- and middle-income countries," *Clin. Integr. Care*, vol. 1, p. 100005, Jul. 2020, doi: 10.1016/j.intcar.2020.100005.

[13] M. Fessina, A. Zaccaria, G. Cimini, and T. Squartini, "Pattern-detection in the global automotive industry: a manufacturer-supplier-product network analysis," *Chaos Solitons Fractals*, vol. 181, p. 114630, Apr. 2024, doi: 10.1016/j.chaos.2024.114630.

[14] A. A. Abioye *et al.*, "A Review on Automotive Industries and Foundries in Nigeria," *IOP Conf. Ser. Mater. Sci. Eng.*, vol. 413, no. 1, p. 012003, Sep. 2018, doi: 10.1088/1757-899X/413/1/012003.

[15] A. S. Slutsky, "History of Mechanical Ventilation. From Vesalius to Ventilator-induced Lung Injury," *Am. J. Respir. Crit. Care Med.*, vol. 191, no. 10, pp. 1106–1115, May 2015, doi: 10.1164/rccm.201503-0421PP.

[16] "Mechanical ventilators for low- and middle-income countries: informing a context-specific and sustainable design - British Journal of Anaesthesia." Accessed: Jun. 01, 2025. [Online]. Available: https://www.bjanaesthesia.org/article/S0007-0912(22)00015-0/fulltext

[17] J. M. Pearce, "A review of open source ventilators for COVID-19 and future pandemics," *F1000Research*, vol. 9, p. 218, 2020, doi: 10.12688/f1000research.22942.2.

[18] C. Dave, P. Cameron, J. Basmaji, G. Campbell, E. Buga, and M. Slessarev, "Frugal Innovation: Enabling Mechanical Ventilation During Coronavirus Disease 2019 Pandemic in Resource-Limited Settings," *Crit. Care Explor.*, vol. 3, no. 4, p. e0410, Apr. 2021, doi: 10.1097/CCE.0000000000000410.

[19] J. B. West, "Robert Hooke: early respiratory physiologist, polymath, and mechanical genius," *Physiol. Bethesda Md*, vol. 29, no. 4, pp. 222–233, Jul. 2014, doi: 10.1152/physiol.00005.2014.
[20] R. M. Kacmarek, "The Mechanical Ventilator: Past, Present, and Future," *Respir. Care*, vol. 56, no. 8, pp. 1170–1180, Aug. 2011, doi: 10.4187/respcare.01420.
[21] "RAMR - Volumen 17, Número3 Avances en la historia de la VMNI. Período de Entreguerras (1919-1939)." Accessed: Jun. 01, 2025. [Online]. Available: https://www.ramr.org/articulos/volumen_17_numero_3/medicina_respiratoria_historia/medicina_respiratoria_historia_avances_en_la_historia_de_la_vmni._periodo_de_entreguerras_1919_1939.php
[22] J. B. West, "The physiological challenges of the 1952 Copenhagen poliomyelitis epidemic and a renaissance in clinical respiratory physiology," *J. Appl. Physiol. Bethesda Md 1985*, vol. 99, no. 2, pp. 424–432, Aug. 2005, doi: 10.1152/japplphysiol.00184.2005.
[23] J. B. West, "The physiological challenges of the 1952 Copenhagen poliomyelitis epidemic and a renaissance in clinical respiratory physiology," *J. Appl. Physiol.*, vol. 99, no. 2, pp. 424–432, Aug. 2005, doi: 10.1152/japplphysiol.00184.2005.
[24] G. Thiéry *et al.*, "FROM MECHANICAL VENTILATION TO INTENSIVE CARE MEDICINE: A CHALLENGE FOR BOSNIA AND HERZEGOVINA," *Bosn. J. Basic Med. Sci.*, vol. 9, no. Suppl 1, pp. S69–S76, Oct. 2009, doi: 10.17305/bjbms.2009.2766.
[25] K. A. Powers and A. S. Dhamoon, "Physiology, Pulmonary Ventilation and Perfusion," in *StatPearls*, Treasure Island (FL): StatPearls Publishing, 2025. Accessed: Jun. 01, 2025. [Online]. Available: http://www.ncbi.nlm.nih.gov/books/NBK539907/
[26] "Lung Gas Exchange - an overview | ScienceDirect Topics." Accessed: Jun. 01, 2025. [Online]. Available: https://www.sciencedirect.com/topics/neuroscience/lung-gas-exchange
[27] S. L. Phyu, C. Turnbull, and N. Talbot, "Basic respiratory physiology," *Medicine (Baltimore)*, vol. 51, no. 10, pp. 679–683, Oct. 2023, doi: 10.1016/j.mpmed.2023.07.006.
[28] E. Atangana and A. Atangana, "Facemasks simple but powerful weapons to protect against COVID-19 spread: Can they have sides effects?," *Results Phys.*, vol. 19, p. 103425, Dec. 2020, doi: 10.1016/j.rinp.2020.103425.
[29] "Pulmonary Compliance - an overview | ScienceDirect Topics." Accessed: Jun. 01, 2025. [Online]. Available: https://www.sciencedirect.com/topics/nursing-and-health-professions/pulmonary-compliance
[30] Z. Edwards and P. Annamaraju, "Physiology, Lung Compliance," in *StatPearls*, Treasure Island (FL): StatPearls Publishing, 2025. Accessed: Jun. 01, 2025. [Online]. Available: http://www.ncbi.nlm.nih.gov/books/NBK554517/
[31] A. M. Joffe and S. A. Deem, "Chapter 7 - Physiologic and Pathophysiologic Responses to Intubation," in *Benumof and Hagberg's Airway Management (Third Edition)*, C. A. Hagberg, Ed., Philadelphia: W.B. Saunders, 2013, pp. 184-198.e4. doi: 10.1016/B978-1-4377-2764-7.00007-5.
[32] A. van Diepen *et al.*, "Evaluation of the accuracy of established patient inspiratory effort estimation methods during mechanical support ventilation," *Heliyon*, vol. 9, p. e13610, Feb. 2023, doi: 10.1016/j.heliyon.2023.e13610.
[33] N. J. Napoli, V. R. Rodrigues, and P. W. Davenport, "Characterizing and Modeling Breathing Dynamics: Flow Rate, Rhythm, Period, and Frequency," *Front. Physiol.*, vol. 12, p. 772295, Feb. 2022, doi: 10.3389/fphys.2021.772295.
[34] S. M. Hickey, A. Sankari, and A. O. Giwa, "Mechanical Ventilation," in *StatPearls*, Treasure Island (FL): StatPearls Publishing, 2025. Accessed: Jun. 01, 2025. [Online]. Available: http://www.ncbi.nlm.nih.gov/books/NBK539742/
[35] T. Bein *et al.*, "The standard of care of patients with ARDS: ventilatory settings and rescue therapies for refractory hypoxemia," *Intensive Care Med.*, vol. 42, no. 5, pp. 699–711, 2016, doi: 10.1007/s00134-016-4325-4.
[36] P. L. Silva and P. R. M. Rocco, "The basics of respiratory mechanics: ventilator-derived parameters," *Ann. Transl. Med.*, vol. 6, no. 19, Art. no. 19, Oct. 2018, doi: 10.21037/atm.2018.06.06.
[37] A. L. Mora Carpio and J. I. Mora, "Positive End-Expiratory Pressure," in *StatPearls*, Treasure Island (FL): StatPearls Publishing, 2025. Accessed: Jun. 01, 2025. [Online]. Available: http://www.ncbi.nlm.nih.gov/books/NBK441904/
[38] S. Mora, F. Duarte, and C. Ratti, "Can Open Source Hardware Mechanical Ventilator (OSH-MVs) initiatives help cope with the COVID-19 health crisis? Taxonomy and state of the art," *HardwareX*, vol. 8, p. e00150, Oct. 2020, doi: 10.1016/j.ohx.2020.e00150.

[39] V. Kumar, R. Kumar, M. Kumar, G. S. Wander, V. Gupta, and A. Sahani, "Recent advances in low-cost, portable automated resuscitator systems to fight COVID-19," *Health Technol.*, vol. 12, no. 1, pp. 181–191, 2022, doi: 10.1007/s12553-021-00629-4.
[40] J. Bonvoisin, T. Buchert, M. Preidel, and R. Stark, "How participative is open source hardware? Insights from online repository mining," *Des. Sci.*, vol. 4, Nov. 2018, doi: 10.1017/dsj.2018.15.
[41] M. L. Ranney, V. Griffeth, and A. K. Jha, "Critical Supply Shortages - The Need for Ventilators and Personal Protective Equipment during the Covid-19 Pandemic," *N. Engl. J. Med.*, vol. 382, no. 18, p. e41, Apr. 2020, doi: 10.1056/NEJMp2006141.
[42] G. Meiry *et al.*, "The rapid development of AmboVent: a simple yet sustainable ventilation solution for use in a pandemic," *Minim. Invasive Ther. Allied Technol. MITAT Off. J. Soc. Minim. Invasive Ther.*, vol. 31, no. 4, pp. 556–566, Apr. 2022, doi: 10.1080/13645706.2021.1881797.
[43] "OEDK - Rice University - ApolloBVM." Accessed: Jun. 01, 2025. [Online]. Available: https://oedk.wildapricot.org/apollobvm
[44] A. Becker, "Rice University engineers design DIY ventilation unit," TMC News. Accessed: Jun. 01, 2025. [Online]. Available: https://www.tmc.edu/news/2020/07/rice-university-engineers-design-diy-ventilation-unit/
[45] C. Galbiati *et al.*, "Mechanical Ventilator Milano (MVM): A Novel Mechanical Ventilator Designed for Mass Scale Production in Response to the COVID-19 Pandemic," *Phys. Fluids*, vol. 33, no. 3, p. 037122, Mar. 2021, doi: 10.1063/5.0044445.
[46] "Ventilators co-designed by a Canadian team led by Queen's Nobel Laureate ready to go | Queen's Gazette." Accessed: Jun. 01, 2025. [Online]. Available: queensu.ca/gazette/stories/ventilators-co-designed-canadian-team-led-queen-s-nobel-laureate-ready-go
[47] Md. H. Imran, R. B. Mahi, R. Saha, M. H. Islam, and I. Mahmud, "NISHASH: A reasonable cost-effective mechanical ventilator for COVID affected patients in Bangladesh," *Heliyon*, vol. 8, no. 5, p. e09400, May 2022, doi: 10.1016/j.heliyon.2022.e09400.
[48] "Mechanical Ventilator Market Size And Share Report, 2030." Accessed: May 29, 2025. [Online]. Available: https://www.grandviewresearch.com/industry-analysis/mechanical-ventilators-market
[49] "Mechanical Ventilators Market Size | Mordor Intelligence." Accessed: May 29, 2025. [Online]. Available: https://www.mordorintelligence.com/industry-reports/mechanical-ventilators-market
[50] P. M. R. https://www.polarismarketresearch.com, "Ventilators Market Size Report, 2022 - 2030," Polaris. Accessed: Jun. 01, 2025. [Online]. Available: https://www.polarismarketresearch.com/industry-analysis/ventilators-market
[51] Y. Wang *et al.*, "The aging lung: microenvironment, mechanisms, and diseases," *Front. Immunol.*, vol. 15, May 2024, doi: 10.3389/fimmu.2024.1383503.
[52] J. Kim, R. L. Heise, A. M. Reynolds, and R. M. Pidaparti, "Aging effects on airflow dynamics and lung function in human bronchioles," *PLOS ONE*, vol. 12, no. 8, p. e0183654, Aug. 2017, doi: 10.1371/journal.pone.0183654.
[53] S. M. Levine and D. D. Marciniuk, "Global Impact of Respiratory Disease," *Chest*, vol. 161, no. 5, pp. 1153–1154, May 2022, doi: 10.1016/j.chest.2022.01.014.
[54] T. Ferkol and D. Schraufnagel, "The global burden of respiratory disease," *Ann. Am. Thorac. Soc.*, vol. 11, no. 3, pp. 404–406, Mar. 2014, doi: 10.1513/AnnalsATS.201311-405PS.
[55] M. Menniti, F. Laganà, G. Oliva, M. Bianco, A. S. Fiorillo, and S. A. Pullano, "Development of Non-Invasive Ventilator for Homecare and Patient Monitoring System," *Electronics*, vol. 13, no. 4, Art. no. 4, Jan. 2024, doi: 10.3390/electronics13040790.
[56] D. Soler-Segovia, V. Guerra-Ruíz, M. Massa, M.-F. Pilia, M.-J. Cruz, and X. Muñoz, "Consequences of climate change for asthma: Reviewing the evidence," *Curr. Opin. Environ. Sci. Health*, vol. 46, p. 100630, Aug. 2025, doi: 10.1016/j.coesh.2025.100630.
[57] G. D'Amato, L. Cecchi, M. D'Amato, and I. Annesi-Maesano, "Climate change and respiratory diseases," *Eur. Respir. Rev.*, vol. 23, no. 132, pp. 161–169, Jun. 2014, doi: 10.1183/09059180.00001714.
[58] K. Iyengar, S. Bahl, Raju Vaishya, and A. Vaish, "Challenges and solutions in meeting up the urgent requirement of ventilators for COVID-19 patients," *Diabetes Metab. Syndr. Clin. Res. Rev.*, vol. 14, no. 4, pp. 499–501, Jul. 2020, doi: 10.1016/j.dsx.2020.04.048.
[59] C. Q. A. Fais and H. T. Moriya, "Premarket and postmarket regulatory challenges for mechanical ventilators: scenario in Brazil and comparison with other countries," *Discov. Public Health*, vol. 21, no. 1, p. 46, Aug. 2024, doi: 10.1186/s12982-024-00176-z.

[60] iHealthcareAnalyst Inc, "Global Mechanical Ventilators Market $9.5 Billion by 2031," iHealthcareAnalyst, Inc. - Healthcare Market Research. Accessed: May 29, 2025. [Online]. Available: https://www.ihealthcareanalyst.com/mechanical-ventilators-market/
[61] A. I. P. Ltd, "Mechanical Ventilator Market to Surpass Market Valuation of US$ 9,668.8 Million By 2032 | Astute Analytica," GlobeNewswire News Room. Accessed: May 29, 2025. [Online]. Available: https://www.globenewswire.com/news-release/2024/02/15/2829952/0/en/Mechanical-Ventilator-Market-to-Surpass-Market-Valuation-of-US-9-668-8-Million-By-2032-Astute-Analytica.html
[62] S. Roy, "Philips to Up Hospital Ventilator Production to 4,000 Units/Week and Launches a New Ventilator at 15,000 Units/Week," Sleep Review. Accessed: May 29, 2025. [Online]. Available: https://sleepreviewmag.com/sleep-treatments/therapy-devices/ventilation-therapy-asv/philips-hospital-ventilator-production-e30/
[63] R. and M. ltd, "Mechanical Ventilators - Market Share Analysis, Industry Trends & Statistics, Growth Forecasts (2025 - 2030)." Accessed: May 29, 2025. [Online]. Available: https://www.researchandmarkets.com/reports/4896228/mechanical-ventilators-market-share-analysis
[64] L. F. Giraldo-Cadavid *et al.*, "The development and implementation of a low-cost mechanical ventilator in a low-middle-income country during the COVID-19 pandemic: The Unisabana-HERONS," *Heliyon*, vol. 10, no. 9, p. e30671, May 2024, doi: 10.1016/j.heliyon.2024.e30671.
[65] V. Krishnamoorthy, M. S. Vavilala, and C. N. Mock, "The need for ventilators in the developing world: An opportunity to improve care and save lives," *J. Glob. Health*, vol. 4, no. 1, p. 010303, Jun. 2014, doi: 10.7189/jogh.04.010303.
[66] J. F. Gieras and J.-X. Shen, *Modern Permanent Magnet Electric Machines: Theory and Control*. Boca Raton: CRC Press, 2022. doi: 10.1201/9781003103073.
[67] "(PDF) An examination of naturalistic Windshield wiper usage." Accessed: Jun. 02, 2025. [Online]. researchgate.net/publication/264439240_An_examination_of_naturalistic_Windshield_wiper_usage
[68] "Design and development of smart automatic windshield wiper ... Pages 1-7 - Flip PDF Download | FlipHTML5." Accessed: Jun. 01, 2025. [Online]. Available: https://fliphtml5.com/lecs/owan/basic
[69] C. Chourpiliadis and A. Bhardwaj, "Physiology, Respiratory Rate," in *StatPearls*, Treasure Island (FL): StatPearls Publishing, 2025. Accessed: Jun. 01, 2025. [Online]. Available: http://www.ncbi.nlm.nih.gov/books/NBK537306/
[70] A. Dileep, "Measurement systems application design", Accessed: Jun. 02, 2025. [Online]. Available: https://www.academia.edu/35554924/Measurement_systems_application_design
[71] *Pilbeam's Mechanical Ventilation*. 2015. Accessed: Jun. 01, 2025. [Online]. Available: https://shop.elsevier.com/books/pilbeams-mechanical-ventilation/cairo/978-0-323-32009-2
[72] J. Kestin, M. Sokolov, and W. A. Wakeham, "Viscosity of liquid water in the range −8 °C to 150 °C," *J. Phys. Chem. Ref. Data*, vol. 7, no. 3, pp. 941–948, Jul. 1978, doi: 10.1063/1.555581.
[73] J. López-Herce and Á. Carrillo, "Ventilación mecánica: indicaciones, modalidades y programación y controles," *An. Pediatría Contin.*, vol. 6, no. 6, pp. 321–329, Dec. 2008, doi: 10.1016/S1696-2818(08)75597-5.
[74] "Regulation - 2017/745 - EN - Medical Device Regulation - EUR-Lex." Accessed: May 29, 2025. [Online]. Available: https://eur-lex.europa.eu/eli/reg/2017/745/oj/eng
[75] "DocsRoom - European Commission." Accessed: May 29, 2025. [Online]. Available: https://ec.europa.eu/docsroom/documents/40941
[76] "IEC 60601-2-12:2001," ISO. Accessed: May 29, 2025. [Online]. Available: https://www.iso.org/standard/23914.html
[77] "Emergency Use Authorization | FDA." Accessed: May 29, 2025. [Online]. Available: https://www.fda.gov/emergency-preparedness-and-response/mcm-legal-regulatory-and-policy-framework/emergency-use-authorization
[78] "Regulation and Prequalification." Accessed: May 29, 2025. [Online]. Available: https://www.who.int/teams/regulation-prequalification/eul
[79] "ISO 14971," *Wikipedia*. Apr. 29, 2025. Accessed: May 29, 2025. [Online]. Available: https://en.wikipedia.org/w/index.php?title=ISO_14971&oldid=1287944145